Urine proteomic characterization of active and recovered COVID-19 patients

Jianping Sun[1†], Jing Wei[2,3†], Haibin Yu[1†], Haidan Sun[4], Xiaoyan Liu[4], Yonghong Zhang[1], Chen Shao[5*], Wei Sun[4*], Jing Zhang[1*], Youhe Gao[2*]
† These authors contributed equally to the work.
* To whom correspondence may be addressed.

1. Beijing Youan Hospital, Capital Medical University, Beijing, People's Republic of China.
2. Department of Biochemistry and Molecular Biology, Beijing Normal University, Gene Engineering Drug and Biotechnology Beijing Key Laboratory, Beijing, China.
3. Department of Pharmacy, Clinical Research Center, Beijing Children's Hospital, Capital Medical University, National Center for Children's Health, Beijing, China.
4. Core Facility of Instrument, Institute of Basic Medical Sciences, Chinese Academy of Medical Sciences, School of Basic Medicine, Peking Union Medical College, Beijing, China.
5. State Key Laboratory of Proteomics, Beijing Proteome Research Center, National Center for Protein Sciences (Beijing), Beijing Institute of Lifeomics, Beijing 102206, China.

Correspondence:
Chen Shao: scshaochen@126.com
Wei Sun: sunwei@ibms.pumc.edu.cn
Jing Zhang: zjyouan@ccmu.edu.cn
Youhe Gao: gaoyouhe@bnu.edu.cn

Abstract

Background: The molecular changes in COVID-19 patients have been reported in many studies. However, there were limited attention has been given to the disease sequelae in the recovered COVID-19 patients.

Methods: Here, we profiled the urine proteome of a cohort of 29 COVID-19 patients in their disease onset and recovery period, including mild, severe, and fatal patients and survivors who recovered from mild or severe symptoms.

Results: The molecular changes in the COVID-19 onset period suggest that viral infections, immune response changes, multiple organ damage, cell injury, coagulation system changes and metabolic changes are associated with COVID-19 progression. The patients who recovered from COVID-19 still exhibited an innate immune response, coagulation system changes and central nervous system changes. We also proposed four potential biomarkers to monitor the whole progression period of COVID-19.

Conclusions: Our findings provide valuable knowledge about the potential molecular pathological changes and biomarkers that can be used to monitor the whole period of COVID-19.

Key words: COVID-19, disease sequelae, urinary proteome, biomarker

Background

The ongoing COVID-19 pandemic, caused by severe acute respiratory syndrome coronavirus 2 (SARS-CoV-2), has led to 754,367,807 confirmed cases and 6,825,461 deaths worldwide as reported by the World Health Organization (WHO) on 6， February 2023, with a tremendous impact on global health and economics. SARS-CoV-2 has been reported to infect multiple organs, including the lung, liver, heart, muscle, gastrointestinal tract, spleen, testis, thyroid and central nervous system[1-4]. Currently, most proteomic studies focus on the molecular changes in COVID-19 patients, such as the immune response, blood coagulation and fibrosis, as well as potential biomarkers for severity evaluation[4-8]. Only limited studies have revealed the molecular changes between active and recovered COVID-19 patients using serum proteomics[9,10]. As up to 87.4% of patients who have recovered from COVID-19 report persistent fatigue and dyspnea[11], there is still an urgent need for a comprehensive understanding of the molecular level changes throughout the entire course of COVID-19 patients.

Urine has been regarded as a promising biomarker source, as it is noninvasive, easily collected and can reflect multiple organ changes[12,13]. Notably, urine samples are less complex than blood samples and carry many proteins, peptides, and amino acids that have not been discovered in blood. Currently, a total of 6085 proteins have been reported to be identified in normal human urine[14]. The urine proteome has been applied to stratify patients with familial Parkinson's disease[15] and to discriminate lung cancer patients from other common tumors[16]. In addition, the urine proteome has also been used to reflect the immune response in moderate and severe COVID-19 patients[17,18] and to identify potential biomarkers to predict patients with mild to severe symptoms[19]. However, the study of biomarkers to monitor the whole process of COVID-19 is still unavailable.

In this study, we presented a urinary proteomic analysis including the entire course of COVID-19 from the onset to the progression and recovery periods. This whole course included a total of six phases, namely, the mild phase (M), the severe phase (S), the fatal phase (F), the mild remission phase (MRE), the severe remission phase (SRE), and the severe return visit phase (SRT). The mass spectrometry-based, data-independent acquisition (DIA) quantitative proteomic approach was performed to analyze urine samples from healthy donors, COVID-19 patients and their recovery period. The altered urine proteins were classified into six categories: virus infection, immune response, organ damage, cell injury, coagulation system changes, and metabolic changes. We also analyzed our urine proteomic data in conjunction with the clinical serum indicators of the COVID-19 patients. Finally, we propose candidate monitoring urine biomarkers for the entire course of COVID-19. These biomarkers can be used not only as diagnostic biomarkers of COVID-19 but also as potential prognostic biomarkers to predict disease recovery. Our data provide valuable knowledge of the molecular changes in the whole period of COVID-19, including the recovery phase, and shed light on the potential biomarkers for monitoring the entire disease course.

Methods

Experimental Design and Statistical Rationale

COVID-19 patients were recruited in Beijing Youan Hospital from January to February 2020. All work performed in this study was approved by the Beijing Youan Hospital Ethics Committee (LL-2020-030-K). Written informed consent was obtained from the patients. Patients were diagnosed with COVID-19 based on the Chinese Government Diagnosis and Treatment Guideline (Trial 5th version) published by the National Health Commission of China (National Health Commission, 2020)[20]. The healthy donors were recruited from health care workers at Beijing Youan Hospital, and none of them had previously been infected with SARS-CoV-2.

SARS-CoV-2-positive patients were enrolled in this study after diagnosis. According to the abovementioned diagnosis standards, these recruited COVID-19 patients were classified into three subgroups: 1) mild-mild symptoms mainly manifested with symptoms of fever, nonpneumonia or mild pneumonia; 2) severe-fulfilled any of the following three criteria: respiratory distress, respiratory rate ($R \geq 30$ times/min); mean oxygen saturation ($\leq 93\%$, resting state); arterial blood oxygen partial pressure/oxygen concentration ($PaO2/FiO2 \leq 300$ mmHg); 3) fatal - fulfilled any of the three criteria: respiratory failure and required mechanical ventilation; shock incidence; admission to the ICU.

In this study, we collected urine samples from a cohort of 29 COVID-19 patients, including 12 patients diagnosed with mild (M) symptoms, 16 patients diagnosed with severe (S) symptoms and 2 patients with fatal (F) outcomes. The 12 mild patients included a total of 19 urine samples for proteomic analysis, namely, 6 mild onset period samples (M), 11 mild remission samples (MRE) and 2 mild return visit samples (MRT). The 16 severe patients included a total of 31 urine samples for proteomic analysis, namely, 10 severe onset period samples (S), 16 severe remission samples (SRE) and 5 severe return visit (SRT) samples. The two fatal patients included 3 fatal onset period urine samples (F). The remission urine samples were taken after the patients tested negative for SARS-CoV-2. Midstream first morning urine was collected from these subjects. After collection, the urine was immediately centrifuged at 5,000 g for 30 min at 4 °C to remove the cell debris and then sterilized at 56 °C to inactivate the virus.

Proteomics sample preparation

Urine samples were prepared using the FASP method [21]with some modifications. Briefly, 4 ml urine from each specimen was reduced with 20 mmol/L dithiothreitol (DTT, Sigma) at 95 °C for 5 min and then alkylated by 50 mmol/L iodoacetamide (IAA, Sigma) for 45 min in the dark. Then, the urine samples were precipitated with six volumes of ethanol at -20 °C overnight. The pellets were dissolved in lysis buffer (8 mol/L urea, 2 mol/L thiourea 50 mmol/L Tris, and 25 mmol/L DTT). The protein amount of each sample was measured using the Bradford method.

A total of 100 μg of protein from each sample was loaded onto a 10 kDa filter device (Pall, Port Washington, NY, USA). After being washed two times with urea buffer (UA, 8 mol/L urea, 0.1 mol/L Tris-HCl, pH 8.5) and 25 mmol/L NH_4HCO_3

solutions, these samples were digested with trypsin at 37 ℃ for 14 h. The digested peptides were desalted using Oasis HLB cartridges (Waters, Milford, MA, USA) and dried by vacuum evaporation (Thermo Fisher Scientific, Bremen, Germany). The peptide concentration was measured using the BCA method.

Spin column peptide fractionation

Digested peptides were dissolved in 0.1% formic acid and diluted to 0.5 μg/μL. A pooled sample (96 μg, 1.5 μg of each sample) from 64 samples was loaded onto a high-pH, reversed-phase fractionation spin column (84868, Thermo Fisher Scientific) to generate a spectral library. Briefly, the spin column was equilibrated with acetonitrile and 0.1% formic acid solution. Then, the sample solution was loaded on the column to elute the "flow-through" fraction, while the water was loaded on the column to elute the "wash" fraction. Next, a step gradient of 8 increasing acetonitrile concentrations (5, 7.5, 10, 12.5, 15, 17.5, 20 and 50% acetonitrile) in a volatile high-pH elution solution was added to the column to elute these peptides into eight different gradient fractions. Finally, the fractionated peptides were evaporated and resuspended in 20 μl of 0.1% formic acid. Two microliters of each fraction was loaded for LC-DDA-MS/MS analysis.

LC–MS/MS analysis

LC–MS/MS data acquisition was carried out on a Orbitrap Fusion Lumos mass spectrometer coupled with an Easy-nLC 1200 system (both from Thermo Scientific). The iRT reagent (Biognosys, Switzerland) was added at a concentration of 1:20 v/v in all peptide samples to calibrate the retention time of extracted peptide peaks. For analysis, 1 μg of peptide from each sample was loaded into a C18 trap column (75 μm * 2 cm, 3 μm, C18, 100 Å) and then separated with a reversed-phase analytical column (100 μm * 100 cm, 2 μm) at a flow rate 1 μL/min with a 120 min gradient (buffer B: 2%–6% for 1 min, 6%–10% for 23 min, 10%–20% for 67 min, 20%–28% for 7 min, 28%–95% for 20 min, and 95%–5% for 2 min). The LC settings were the same in both DDA-MS and DIA-MS modes to maintain a stable retention time. Ten fractions from spin column separation were analyzed with mass spectrometry in DDA mode to generate the spectral library. The MS data were acquired in high-sensitivity mode. A full MS scan was acquired in a 350-1,500 m/z range with the resolution set to 120,000. The MS/MS scan was acquired in Orbitrap with a resolution of 30,000. The HCD collision energy was set to 32%. The AGC target was set to 5e4, and the maximum injection time was 45 ms.

Then, 54 individual urine samples were analyzed in DIA-MS mode. The variable isolation window of the DIA method with 26 windows was developed for DIA acquisition. Positive ion mode was set to 3000 V. The full scan was set at a resolution of 120,000 with a m/z range from 350 to 1,200, and the DIA scan was set at a resolution of 30,000. The maximum injection time was 50 ms. The HCD collision energy was set to 32%. To ensure the quality of the data, the pooled peptides of all samples were used to ensure the stability of the instrument. A single pooled DIA analysis was run among after every 7-9 samples to serve as the technical replicate

quality control. Different groups of samples were acquired in a random order to reduce system bias during mass spectrometry analysis.

Mass spectrometry data processing

The MS data of the fractionated pools (DDA MS data, 10 COVID-19 pool urine and 15 human normal pool urine) and the single-shot subject samples (DIA MS data, 64 COVID-19 samples and 8 quality control samples) were used to generate a DDA library and direct DIA library, respectively, which were computationally merged into three cohort-specific hybrid libraries using Spectronaut (v14.0.200409.43655, Biognosys AG). The searched database included the human SwissProt database (released in May 2019, containing 20,421 sequences), the SARS-CoV-2 proteome database containing 14 protein sequences and the 11 peptide iRT sequence. Searches used carbamidomethylation as a fixed modification and acetylation of the protein N-terminus and oxidation of methionines as variable modifications. The trypsin/P proteolytic cleavage rule was used, permitting a maximum of 2 missed cleavages and a minimum peptide length of 7 amino acids. The Q-value cutoffs for both library generation and DIA analyses at the peptide and protein levels were set to 0.01.

A total of 8 QC samples and 64 DIA samples were imported into Spectronaut Pulsar X with default settings. The optimal XIC extraction window was determined according to the iRT calibration strategy. Cross-run normalization was performed to calibrate systematic variance in LC–MS performance, and local normalization based on local regression was used [22]. Protein inference was performed using the implemented IDPicker algorithm [23]. All results were then filtered by a Q value less than 0.01 (corresponding to an FDR of 1%). The peptide intensity was calculated by summing the peak areas of the respective fragment ions for MS2. Protein intensity was calculated by summing the respective peptide intensity.

Statistical analysis

To analyze the proteomic data, we first used the sequential-KNN method to impute the missing value of QC samples[24]. Missing values larger than 50% were removed for later analysis. The QC samples were used as technical replicates to evaluate the stability of mass spectrometry. Then, the 64 DIA samples were imputed as the healthy control group, the disease group, and the recovery group.

For later analysis, we normalized the protein abundance by log2 transformation for P value analysis. Differential urinary proteins in the six periods of COVID-19 were compared with the healthy control group using the following criteria: fold change ≥ 2 or ≤ 0.5; comparison between two groups were conducted using a two-sided, unpaired t test; and P values of group differences were adjusted by the Benjamini and Hochberg method[25]. Group differences resulting in adjusted P values <0.05 were considered statistically significant. All results are expressed as the mean ± standard deviation.

Bioinformatics analysis

Protein interaction network analysis was performed using the STRING database (https://string-db.org/cgi/input.pl) and visualized by Cytoscape (V.3.7.1) [26]. The canonical pathways as well as disease and function categories were enriched using

IPA software (Ingenuity Systems, Mountain View, CA). The bubble figures were visualized by the Wu Kong platform (https://www.omicsolution.org/wkomics/main/).

Biomarker screening

The potential urine biomarkers for monitoring were selected according to the following criteria: i) differential proteins were present in all three active phases, in the M and S phases, or in the S and F phases of COVID-19; ii) differential proteins were upregulated/downregulated gradually in the active phase but changed reversely in the recovery period; iii) differential proteins were not significantly different in the recovery stages compared with the healthy control; and iv) the potential monitoring biomarkers were associated with the molecular changes of COVID-19 patients.

Results

Study design and clinical characteristics

We collected urine samples from a cohort of 29 COVID-19 patients, including 12 patients diagnosed with mild (M) symptoms, 16 patients diagnosed with severe (S) symptoms and 2 patients with fatal (F) outcomes. Healthy control urine samples were collected from 11 healthy (H) donors at Beijing Youan Hospital. The patients in the M and S groups survived COVID-19 and were discharged from the hospital. Of note, the 12 mild patients included a total of 19 urine samples for proteomic analysis, namely, 6 mild onset period samples (M), 11 mild remission samples (MRE) and 2 mild return visit samples (MRT). The 16 severe patients included a total of 31 urine samples for proteomic analysis, namely, 10 severe onset period samples (S), 16 severe remission samples (SRE) and 5 severe return visit (SRT) samples. The two fatal patients included 3 fatal onset period urine samples (F) (Figure 1). The remission urine samples were taken after the patients tested negative for SARS-CoV-2.

The detailed patient descriptions in their onset and recovery phases are shown in Table 1. In addition, we also analyzed 28 clinical measurements of the COVID-19 patients in their onset and recovery period (Figure S1, Table S1). These clinical indicators cover liver function, kidney function, immune and inflammatory changes, myocardial function and coagulation functional changes. As shown in Figure S1, we noticed that the clinical indicators of liver function, such as AST, ALT, DBIL and TBIL, were upregulated in the active period but downregulated in the recovery period. Immune and inflammatory indicators, such as N and WBC, were upregulated in the active period but downregulated in the recovery period. LYMPH exhibited the reverse change compared with N and WBC. Coagulation function indicators such as TT and myocardial function indicators such as CK-MB and TnI were upregulated in the active phase of COVID-19 but downregulated in the recovery phase. When compared with the M or S patients, the fatal patients showed significant suppression of lymphocyte count, as well as increases in neutrophil count, WBC, AST, CK-MB, MYO, TnI, TT and HGB. When compared with the COVID-19 patients in their onset period, we noticed that the PLT, LYMPH, MONO and AST showed the reversed change in their recovery phase.

Quantitative urine proteome profiling of COVID-19 patients in the disease and recovery stages

We used a data-independent acquisition (DIA) strategy and liquid chromatography/tandem mass spectrometry (LC–MS/MS) to analyze the urine samples. A total of 3367 protein groups were identified from 64 urine samples with a false discovery date (FDR) of less than 1% at both the peptide and protein levels. A total of 2950 protein groups were identified with at least two peptides. The number of protein groups in each sample is presented in Figure S2A. No SARS-CoV-2 proteins were identified from 64 urine samples. The median coefficient of variance (CV) and the correlation of QC samples indicated the great consistency and reproducibility of our data (Figure S2B, S2C). A total of 2574 protein groups of the healthy group, COVID-19 group and recovery group were retained, as their missing values were less than 50% (Table S2). The t-distributed stochastic neighbor embedding (t-SNE) analysis of the 2574 protein groups showed clear stratification between the COVID-19 patients, the recovery group and the healthy group, while the recovery group was more similar to the healthy control (Figure 2A).

Differential proteins were all compared with the healthy group with fold change≥2 and Benjamini–Hochberg (B-H) adjusted p value<0.05. Finally, there were 291, 601, 987, 245, 336 and 213 differentially expressed proteins in the M, S, F, MRE, SRE and SRT groups, respectively (Table S2). Pearson correlation analysis between the differentially expressed proteins in the M, S and F phases and the 28 clinical indicators was performed. Finally, 456 differentially expressed proteins showed a significant correlation with 26 clinical indicators (Figure 2B). These clinical indicators, including the liver, kidney, heart, immune response and coagulation changes, were subgrouped into two clusters. Some clinical indicators, including myocardial function, liver function, kidney functions and a few immune functions, exhibited a positive correlation with our differential urinary proteins, while some other clinical indicators, such as LYMPH, MONO, RBC and HGB, showed a negative correlation with our differential urinary proteins. Our results indicated that our urine proteome changes are highly associated with clinical indicators, such as abnormal liver and kidney function, myocardial abnormalities, disturbances in blood coagulation and abnormal immune or inflammatory changes.

The differential urinary proteins of the six groups were then enriched by the IPA database to reveal the molecular landscape associated with SARS-CoV-2 infections. The enriched canonical pathways as well as the disease and biofunctions were classified into six clusters to reveal the whole process changes in COVID-19 patients in their onset and recovery period. These six clusters included viral infection changes, immune response changes, multiple organ damage, cell injury, coagulation system changes and metabolic changes.

Viral infection changes

The IPA database was used to enrich the related viral infection changes of six periods of COVID-19. The viral infection molecular changes in COVID-19 patients in their onset and recovery periods are presented in Figure 3A. The majority of these molecular changes, such as viral infection, infection of cells, infection by SARS/RNA/coronavirus and the coronavirus replication pathway, are active in the disease phase of COVID-19. Pathways such as viral infection, infection by SARS

coronavirus/RNA virus/coronavirus and the coronavirus replication pathway were active in the three active phases of COVID-19, and the active extent was associated with the severity of COVID-19.

There were 21 differential proteins involved in the coronavirus replication pathway and the coronavirus pathogenesis pathway (Figure 3B). We noticed that cathepsin L1 (CTSL), which is involved in the coronavirus replication pathway, was significantly upregulated in the fatal phase of COVID-19. Transmembrane protease serine 2 (TMPRSS2) and angiotensin-converting enzyme 2 (ACE2) were enriched in coronavirus replication and the coronavirus pathogenesis pathway (Figure 3C). Of note, various 40S ribosomal proteins such as RPSA, RPS12, RPS3A, RPS8, RPS25 and RPS28, were enriched in the coronavirus pathogenesis pathway, indicating that these 40S ribosomal proteins may contribute to the inhibition of the translation system in COVID-19 patients.

Immune response changes

We found that most immune cells, such as phagosomes, macrophages, monocytes, NK cells, T cells, leukocytes, B cells and neutrophils, were enriched in the disease period of COVID-19, while phagosome maturation was still present in the SRE phase of patients. In addition, immune responses, such as cytokines, cell and humoral immunity, innate immunity and some immune-related signaling pathways, were found to be associated with the progression of COVID-19, while innate immunity, such as the complement system, was still present in the SRT phase of severe patients when they recovered from COVID-19 (Figure 3D). In addition, we classified the immune-related urine differential proteins into seven clusters according to the ImmPort database (Figure 3E). Most of these immune-associated differential urine proteins were upregulated gradually, especially in the fatal phase of COVID-19, and decreased in the recovery stages. These results indicated that the immune response is active in the onset period of COVID-19 patients, which is consistent with disease progression and may still be present when they test negative for SARS-CoV-2 infections.

As the cytokine storm contributes to the majority of deaths from COVID-19, we then focused on the common pathways associated with cytokines. A total of 15 common differential proteins associated with the cytokine pathways were identified both in the IPA and ImmPort databases (Figure S3A). We also evaluated a total of 48 cytokine concentrations in the serum of these COVID-19 patients during both the disease period and the recovery period. Serum samples from fatal patients were lacking, as most of the serum samples were collected from COVID-19 patients in the early period of the pandemic outbreak, and the most important job was to save patients' lives at that time. As shown in Figure S3B, the levels of the representative eotaxin, IFN-α2, interleukins (IL-1α, IL-5, IL-6, IL-10), monocyte chemoattractant protein-1 (MCP-1) and monocyte chemoattractant protein-3 (MCP-3) increased significantly in the M and/or S phases of COVID-19 and were downregulated in the recovery periods.

Changes in multiple organs

To estimate the potential organ damage of COVID-19, we enriched differential proteins associated with multiple organs, including brain, heart, lung, liver, kidney and muscle damage, according to the IPA database (Table S3I).

We first compared the differential urine proteins associated with damage to the heart, kidney, lung and liver to the corresponding autopsy results of COVID-19 patients [4] and selected urine proteins with the same fold change (Figure 4A). We also noticed that the neurological system showed a strong association with the disease period of COVID-19 patients and may still be present in their recovery period (Figure 4B). Finally, digestive system and muscle damage were also found according to our results. Digestive system damage appeared not only in severe and fatal patients with COVID-19 but also in the recovery SRE phase. Taking these potential damages into consideration, we found that most of them appeared in the severe and fatal phases, while some of them were still present in the SRE phase, indicating that potential organ damage may still be present in the recovery phase of COVID-19.

Coagulation system changes cell injury

Coagulation system changes appear not only in the disease period of COVID-19 patients but also in their recovery phase (Figure 4C). Various enriched functional lists, such as the coagulation system, thrombus, blood clot and degranulation of blood platelets, were associated with the progression of COVID-19. Notably, we noticed that the coagulation system, intrinsic/extrinsic prothrombin activation pathway and accumulation of blood cells were still present in the SRE phase of patients, indicating that abnormal coagulation may still exist after a negative nucleic acid test. There were 18 differential proteins participated in coagulation system changes (Figure 4D). Interestingly, four differential proteins, urokinase-type plasminogen activator (PLAU), kininogen-1 (KNG1), plasma serine protease inhibitor (SERPINA5) and thrombomodulin (THBD), were downregulated in the disease period but upregulated in the recovery period.

Cell injury and Metabolic changes

The majority of pathways associated with cell injury, such as tight junction signaling, the protein ubiquitination pathway, Myc-mediated apoptosis signaling and the ferroptosis signaling pathway, showed a strong association with the severity of COVID-19 (Figure 4E). HIF-1α signaling was active in the severe and fatal phases of patients in our results.

Changes in amino acids, nuclear acids, glucose and fatty acids were observed in the disease period of patients. We found that amino acid degradation appeared in most of the amino acid metabolism pathways. Of note, thyroid hormone biosynthesis appeared only in the MRE and SRE phases in COVID-19 patients, while the mevalonate pathway I was found to exist in fatal COVID-19 patients. Lipid metabolism plays a crucial role in viral infections, while viruses can use the host lipid machinery to support their life cycle and to impair the host immune response. Therefore, the altered expression of mevalonate pathway-related genes induced by SARS-CoV-2 will ensure their survival and spread in host tissue[27] (Figure 4F).

Potential urine biomarkers to monitor the whole period of COVID-19.

To identify potential specific urine proteins monitoring the whole period of COVID-19, we clustered the 1186 differential proteins in the disease active period into 9 significant discrete clusters with the quantified normalized abundance through mFuzz[28]. According to the previous criteria, we chose Cluster 5 and Cluster 7 for further selection (Figure 5A). Finally, superoxide dismutase [Cu-Zn] (SOD1) and complement factor B (CFB) in Cluster 7 and kininogen-1 (KNG1) and pro-epidermal growth factor (EGF) in Cluster 5 were selected as potential biomarkers for monitoring the whole process of COVID-19 (Figure 5B). SOD1 participates in the superoxide radical degradation pathway, which is categorized as a metabolic change, while CFB participates in the complement system, which is categorized as an immune response in COVID-19 patients. KNG1 and EGF were associated with coagulation changes and immune response changes, as we mentioned before. We also identified another 24 differential proteins, as they also exhibited great differentiation ability in the three active stages of COVID-19 but without systematic molecular functions, as we presented above (Figure S4).

The four candidate monitoring biomarkers (SOD1, CFB, EGF, and KNG1) were then evaluated in 4 mild and 6 severe patients, as these 10 patients had a complete timeline in their onset and recovery period (Figure 5C). The expression of KNG1 and EGF was upregulated, while SOD1 and CFB expression was downregulated in the recovery phase of the 4 mild and 6 severe patients compared with their onset period, indicating great potential monitoring functions as biomarkers.

Finally, we also tried to identify potential diagnostic urine biomarkers in the M, S and F phases of COVID-19 patients. The STRING database was used to generate the PPI network of the DEPs in these three disease phases. Then, the MCC method in the cytoHubba module of CytoScape was used to identify the top 10 hub proteins in the three disease phases (Figure 5D). The area under the curve (AUC) was calculated according to the ROC curve. Interestingly, we found that KNG1 appeared as a hub protein in all three disease periods, with an AUC larger than 0.98 (Figure S5). This result indicated that KNG1 can not only be a potential diagnostic urine biomarker in the M phase of COVID-19 but can also be used as a disease monitoring biomarker in the whole period of COVID-19.

Discussion

The urine proteome has been applied in various aspects of COVID-19, such as to uncover the immune response[29] and identify signaling pathways and therapeutic options[30]. In this study, we focused on the urine proteome changes of the entire course in COVID-19 patients from their onset to the progression and recovery periods, and try to identify potential biomarkers to diagnose and predict COVID-19 recovery.

The urine proteome can reflect viral infection changes. We noticed that cathepsin L1 (CTSL), which is involved in the coronavirus replication pathway, was significantly upregulated in the fatal phase of COVID-19. CTSL is considered the serine protease of SARS-CoV-2 in the endosomal pathway and mediates the cleavage of the S1 subunit of the coronavirus surface spike glycoprotein[31]. Since this cleavage is necessary for coronavirus entry into human host cells, virus and host cell endosome membrane fusion, and viral RNA release for the next round of replication,

the inhibitor of CTSL has been proven to be an effective treatment option for COVID-19 by blocking virus entry[31-33]. CTSL has also been reported to be upregulated in the lung as a potential receptor for virus entry[4]. Transmembrane protease serine 2 (TMPRSS2) and angiotensin-converting enzyme 2 (ACE2) were enriched in coronavirus replication and the coronavirus pathogenesis pathway. It has been reported that SARS-CoV-2 uses the SARS-CoV receptor ACE2 for entry and the serine protease TMPRSS2 for S protein priming, while the TMPRSS2 inhibitor might constitute a treatment option for clinical use by blocking virus entry[34,35]. In addition, as SARS-CoV-2 nonstructural protein 1 (Nsp1) was reported to inhibit protein translation of model human and SARS-CoV-2 messenger RNAs (mRNAs) by specifically binding to the small (40S) ribosomal subunit[36-38], we therefore suppose that these 40S ribosomal proteins may contribute to the inhibition of the translation system in COVID-19 patients.Interestingly, we still noticed that the coronavirus replication pathway, the coronavirus pathogenesis pathway and viral infection were enriched in the three recovery phases of COVID-19 patients despite the negative SARS-CoV-2 test. We therefore suppose that this may be due to the extremely limited number of viruses that cannot reach the standard of the nucleic acid test. It is worth noting that there were still some patients who were reported to test positive when they recovered from COVID-19.

The urine proteome can reflect immune response changes. The Interleukin-1 receptor antagonist protein (IL1RN) was reported to be a potential therapeutic method in acute hyperinflammatory respiratory failure in COVID-19 patients [39]. Similarly, the placenta growth factor (PGF) was reported to have mitogenic, angiogenic, and immunoregulatory properties, enhancing cellular survival, and is involved in host defensive mechanisms, which play an important role in adapting the host to newer infections, making it a promising therapeutic candidate against the COVID-19 virus[40]. Tumor necrosis factor receptor superfamily member 1A (TNFRSF1A) is an immune-based biomarker associated with mortality in COVID-19 patients[41]. Interleukin-18 (IL-18) was reported to be associated with other inflammatory markers and to reflect disease severity[42]. The antagonist of interleukin-6 receptor (IL-6R) can effectively block the IL-6 signal transduction pathway, making it an effective drug for patients with severe COVID-19[43-45]. Azurocidin (AZU1) was found to be significantly altered in naso-oropharyngeal samples of SARS-CoV-2 patients[46]. IL-1α is a ubiquitous and pivotal proinflammatory cytokine that is central to the pathogenesis of numerous conditions characterized by organ or tissue inflammation, including the complex multifactorial COVID-19[47]. IL-6 and IL-10 have been reported as predictors for the fast diagnosis of patients with a higher risk of disease deterioration[48]. MCP-1 and MCP-3 were reported to be biomarkers associated with the severity of COVID-19, which can be related to the progression and risk of death in COVID-19 patients[49,50]. Notably, we found that four urine differential proteins were common to these 48 cytokine-associated proteins, namely, IL1RN, IL-18, EGF and fractalkine (CX3CL1). IL-18 overproduction was reported to participate in the cytokine storm of COVID-19, causing an exaggerated inflammatory burden and leading to tissue injury[51]. Interestingly, we found that EGF was downregulated in

the disease period of COVID-19 both in serum and urine samples but upregulated in the recovery phase. Epidermal growth factor receptor (EGFR) was reported to be upregulated significantly in lung fibrosis tissue[52], while inhibiting EGFR signaling may prevent an excessive fibrotic response to SARS-CoV disease[53]. In addition, EGFR was also regarded as one of the pivotal targets of puerarin in the treatment of COVID-19[54] (Figure 3F). We therefore suppose that the downregulation of EGF in serum and urine may be associated with the severe progression of COVID-19.

We also found that urine proteome may reflect potential organ damage. Vasogenic edema with mild infiltration of inflammatory cells and myocardial cell edema were the major pathological changes that were observed in the hearts of COVID-19 patients. As an inflammatory mediator, matrix metalloproteinase-9 (MMP9) was found to be elevated in the heart and liver of COVID-19 patients and was reported to facilitate matrix degradation and contribute to inflammatory cell invasion[55]. In addition, MMP-9 was also reported as an early indicator of respiratory failure in COVID-19 patients[56]. Lung fibrosis is the most significant pathologic injury in the lungs of COVID-19 patients, accompanied by fibrous exudation, hyaline membrane formation and alveolar space collapse[57]. The immunoglobulin gamma Fc receptor II-a (FCGR2A) was reported to be associated with COVID-19 susceptibility and upregulated in the lung tissue of COVID-19 patients[4,58].The enriched disease and biofunctions associated with brain damage, such as amyloidosis, progressive encephalopathy, Alzheimer's disease (AD), dementia and brain lesions, were increasingly significant, consistent with the progression of COVID-19. The SARS-CoV-2 virus was reported to accelerate the pathogenesis of prion disease[59]. In addition, it has been reported that AD, Parkinson's disease (PD), and dementias are associated with more complicated clinical courses and poorer outcomes in COVID-19 patients[60]. The above results indicated that COVID-19 may deteriorate some brain diseases, such as AD and dementia. Notably, there is increasing evidence that SARS-CoV-2 contributes to a number of neurological issues, including anosmia, seizures, stroke, confusion, encephalopathy, and total paralysis[61,62]. In addition, COVID-19 patients in the intensive care unit (ICU) have neurological deficits at a higher risk of mortality[63], and when they leave the ICU, they may potentially be at higher risk for long-term residual neuropsychiatric and neurocognitive conditions[64,65]. Additionally, the enriched axonal guidance signaling in our results has been reported to promote the rapid spread of the virus from neurons to neurons[66]. As ACE2 was found to be highly expressed in gastrointestinal epithelial cells, gastrointestinal symptoms such as diarrhea, vomiting, and abdominal pain were also reported in some COVID-19 patients[67]. Muscle damage, such as the cell movement of muscle cells, motor dysfunction or movement disorder, and neuromuscular disease, were found to be associated with COVID-19 progression in our results. It has been reported that the COVID-19 pandemic has the potential to disproportionately and severely affect patients with neuromuscular disorders[68]. In addition, myalgia was reported to be described among the common symptoms of COVID-19 after fever, cough, and sore throat, and the duration of myalgia may be related to the severity of COVID-19[69].

The urine proteome can reflect cell injury. Autophagy, the protein ubiquitination pathway and apoptosis signaling are common mechanisms of cell death. Targeting the mechanisms of autophagy was reported as an alternative therapeutic approach for COVID-19, while the clinical decision to inhibit or activate autophagy should depend on the underlying context of the pathological timeline of COVID-19[70]. The ubiquitin modifications can regulate the innate immune response by affecting regulatory proteins, either by altering their stability via the ubiquitin proteasome pathway or by directly regulating their activity. As the intrinsic deubiquitinating activities of papain-like protease (PLP), which is encoded by coronaviruses, antagonize the host's immune response, PLP inhibitors were reported to show promising results as an antiviral therapy in vitro[71]. Furthermore, it has been reported that SARS-CoV-2 infection not only activates apoptosis in lymphocytes, causing lymphopenia[72], but also activates caspase-8 to trigger cell apoptosis and inflammatory cytokine processing in lung epithelial cells[73]. Notably, the ferroptosis signaling pathway was found to be upregulated in fatal COVID-19 patients and did not appear in the recovery phase of COVID-19 patients, which was consistent with the blood single-cell results of COVID-19 patients[74]. Tight junction signaling was associated with the severity of COVID-19 in our results. As tight junctions were reported to exist between epithelial cells in many organs, such as the lung, intestine, kidney and brain[75-77], the disruption of tight junction complexes is the major cause of epithelial barrier breakdown during virus infection[78]. It has been reported that the activation of the HIF-1α signaling pathway under severe hypoxic conditions will induce the activation of proinflammatory cytokine expression and the subsequent inflammation process and cytokine storm phase of COVID-19, which is consistent with our results[79].

The urine proteome can reflect coagulation system changes. PLAU was reported as a thrombolytic agent to positively resolve existing thrombi by accelerating the activity of plasmin[80]. According to the UniProt database, kininogens are inhibitors of thiol proteases, and high-molecular-weight (HMW)-kininogen inhibits the thrombin- and plasmin-induced aggregation of thrombocytes. We therefore suppose that it is reasonable for the downregulation of KNG1 in the disease period of COVID-19 patients. As a member of the serine protease inhibitor family (serpin), antithrombin was reported to be an important protease inhibitor of thrombin and factor Xa[81]. Additionally, THBD was reported to play a vital role in maintaining intravascular patency due to its anticoagulant, anti-inflammatory, and cytoprotective properties[82].

The urine proteome can reflect metabolic changes. The inhibition of the ARE-mediated mRNA degradation pathway, regulation of eIF4 and p70S6K signaling, EIF2 signaling and p70S6K signaling were reported to be translation-associated pathways[4].The reduction in tryptophan degradation was reported to be significantly associated with respiratory severity and correlated with inflammation in COVID-19 patients[83].Thyroid hormones play a key role in modulating metabolism and the immune system. Although thyroid function tests in survivors of COVID-19 have been reported to return to normal at baseline[84], it

cannot be ignored that thyroid function still needs to be considered according to our results. The dysregulated glucose metabolism in severe COVID-19 suggests that SARS-CoV-2 pathogenesis involves a novel interplay with glucose metabolism[85]. Glucose metabolism was found to be dysregulated in the disease period of COVID-19 patients in our results. It has been reported that the upregulation of glucocorticoid receptor alpha appeared in COVID-19 patients[86]. In addition, in a SARS-CoV-2 infection asymptomatic ferret model, the pentose phosphate pathway was also observed in nasal wash samples using a metabonomic method[87].

There are some limitations in our study. First, all of the samples were collected from the patients in the early period of COVID-19 outbreak. Due to the priority to save patients' lives at that time, the number of urine samples were limited and small. A larger number of samples were needed to validate these potential biomarkers in future research. Another possible drawback of this study is that different therapeutic strategies used during the treatment of different patients might affect the results, although the protein alterations uncovered here are quite consistent in different cohorts. Finally, the detailed roles of biomarker proteins such as EGF, KNG1, CFB and SOD1 require further investigation or experimentally validated.

Conclusion

In summary, our study provides the whole system molecular changes of six aspects in COVID-19 patients ranging from the mild period to the severe return visit period (Figure 6). The coronavirus replication/pathogenesis pathway, the immune response changes and the coagulation system changes are associate with the severity of COVID-19 disease. The brain damage as well as the central nervous system changes are also enriched based on our urine proteome data. We also provide potential urine protein biomarkers for monitoring the whole process of COVID-19 including the different stages of active and recovery period. Our finding may provide useful monitoring and therapeutic strategies in the ongoing battle against COVID-19 pandemic.

List of abbreviations

LC-MS/MS: liquid chromatography-tandem mass spectrometry; BMI: body mass index; CI: confidence interval; CV: coefficient of variation; eGFR: estimated glomerular filtration rate; FABP5: fatty acid binding protein 5; FASP: filter-aided sample preparation; QC: quality control; RI: reference interval; ROC: receiver operation curve; COVID-19: Corona Virus Disease 2019; SARS-CoV-2: severe acute respiratory syndrome coronavirus 2; MRE: mild remission; SRE: severe remission; SRT: severe return visit; DIA: data-independent acquisition.

Funding

This work was supported by the National Key Research and Development Program of China (2018YFC0910202 and 2016YFC1306300); the Fundamental Research Funds for the Central Universities (2020KJZX002); the Beijing Natural Science Foundation (7172076); the Beijing Cooperative Construction Project (110651103); the Beijing Normal University (11100704); the Peking Union Medical College Hospital (2016-2.27); and the Beijing Youan Hospital project for COVID-19

(BJYAYY-2020PY-04); National S & T major project for infectious diseases control(2017ZX10202102-003-003).

Availability of data and materials

The mass spectrometry proteomics data have been deposited to the ProteomeXchange Consortium (http://proteomecentral.proteomexchange.org) via the iProX partner repository with the dataset identifier.

Author contributions

Conceptualization: Y.G, C.S, W.S, J.Z, Methodology: J.S, J.W, H.Y, H.S, X.L, Investigation: J.S, Y.Z, H.Y, Visualization: J.W, Supervision: Y.G, C.S, W.S, Writing—original draft: J.W, Y.G, C.S, W.S, Writing—review & editing: J.W, Y.G, C.S, W.S.

Declarations

Ethics approval and consent to participate

COVID-19 patients were recruited in Beijing Youan Hospital from January to February 2020. All work performed in this study was approved by the Beijing Youan Hospital Ethics Committee (LL-2020-030-K). Written informed consent was obtained from the patients. Patients were diagnosed with COVID-19 based on the Chinese Government Diagnosis and Treatment Guideline (Trial 5th version) published by the National Health Commission of China (National Health Commission, 2020)[20]. The healthy donors were recruited from health care workers at Beijing Youan Hospital, and none of them had previously been infected with SARS-CoV-2.

Consent for publication

Not applicable

Competing interests

The authors declare no competing interests.

References

1. De Felice FG, Tovar-Moll F, Moll J, et al. Severe Acute Respiratory Syndrome Coronavirus 2 (SARS-CoV-2) and the Central Nervous System. Trends Neurosci. 2020 Jun;43(6):355-357.
2. Varga Z, Flammer AJ, Steiger P, et al. Endothelial cell infection and endotheliitis in COVID-19. Lancet. 2020 May 2;395(10234):1417-1418.
3. Zhang C, Shi L, Wang FS. Liver injury in COVID-19: management and challenges. Lancet Gastroenterol Hepatol. 2020 May;5(5):428-430.
4. Nie X, Qian L, Sun R, et al. Multi-organ proteomic landscape of COVID-19 autopsies. Cell. 2021 Feb 4;184(3):775-791.e14.
5. Hou X, Zhang X, Wu X, et al. Serum Protein Profiling Reveals a Landscape of Inflammation and Immune Signaling in Early-stage COVID-19 Infection. Mol Cell Proteomics. 2020 Nov;19(11):1749-1759.
6. Shen B, Yi X, Sun Y, et al. Proteomic and Metabolomic Characterization of COVID-19 Patient Sera. Cell. 2020 Jul 9;182(1):59-72.e15.

7. Shu T, Ning W, Wu D, et al. Plasma Proteomics Identify Biomarkers and Pathogenesis of COVID-19. Immunity. 2020 Nov 17;53(5):1108-1122.e5.
8. Liu Y, Song L, Zheng N, et al. A urinary proteomic landscape of COVID-19 progression identifies signaling pathways and therapeutic options. Sci China Life Sci. 2022 Mar 10:1-15.
9. Chen Y, Yao H, Zhang N, et al. Proteomic Analysis Identifies Prolonged Disturbances in Pathways Related to Cholesterol Metabolism and Myocardium Function in the COVID-19 Recovery Stage. J Proteome Res. 2021 Jul 2;20(7):3463-3474.
10. Leng L, Li M, Li W, et al. Sera proteomic features of active and recovered COVID-19 patients: potential diagnostic and prognostic biomarkers. Signal Transduct Target Ther. 2021 Jun 3;6(1):216.
11. Carfì A, Bernabei R, Landi F. Persistent Symptoms in Patients After Acute COVID-19. Jama. 2020 Aug 11;324(6):603-605.
12. Zou L, Sun W. Human urine proteome: a powerful source for clinical research. Advances in experimental medicine and biology. 2015;845:31-42.
13. Rodriguez-Suarez E, Siwy J, Zurbig P, et al. Urine as a source for clinical proteome analysis: from discovery to clinical application. Biochimica et biophysica acta. 2014 May;1844(5):884-98.
14. Zhao M, Li M, Yang Y, et al. A comprehensive analysis and annotation of human normal urinary proteome. Sci Rep. 2017 Jun 8;7(1):3024.
15. Virreira Winter S, Karayel O, Strauss MT, et al. Urinary proteome profiling for stratifying patients with familial Parkinson's disease. EMBO Mol Med. 2021 Mar 5;13(3):e13257.
16. Zhang C, Leng W, Sun C, et al. Urine Proteome Profiling Predicts Lung Cancer from Control Cases and Other Tumors. EBioMedicine. 2018 Apr;30:120-128.
17. Tian W, Zhang N, Jin R, et al. Immune suppression in the early stage of COVID-19 disease. Nat Commun. 2020 Nov 17;11(1):5859.
18. Xiaojie Bi WL, Xuan Ding, Shuang Liang, Yufen Zheng, Xiaoli Zhu, Sheng Quan, Xiao Yi, Nan Xiang, Juping Du, Haiyan Lyu, Die Yu, Chao Zhang, Luang Xu, Weigang Ge, Xinke Zhan, Jiale He, Zi Xiong, Shun Zhang, Yanchang Li, Ping Xu, Guangjun Zhu, Donglian Wang, Hongguo Zhu, Shiyong Chen, Jun Li, Haihong Zhao, Yi Zhu, Huafen Liu, Jiaqin Xu, Bo Shen, Tiannan Guo. Proteomic and metabolomic profiling of urine uncovers immune responses in patients with COVID-19. CEL REP. 2021;S2211-1247(21):01783-6.
19. Li Y, Wang Y, Liu H, et al. Urine proteome of COVID-19 patients. Urine (Amst). 2020;2:1-8.
20. PRC) NNHCot. Diagnosis and Treatment Protocol for COVID-19 (Trial Version 5). http://www.nhc.gov.cn/jkj/s3577/202002/a5d6f7b8c48c451c87dba14889b30147.shtml. 2020.
21. Wisniewski JR, Zougman A, Nagaraj N, et al. Universal sample preparation method for proteome analysis. Nat Methods. 2009 May;6(5):359-62.
22. Callister SJ, Barry RC, Adkins JN, et al. Normalization approaches for removing systematic biases associated with mass spectrometry and label-free proteomics. J Proteome Res. 2006 Feb;5(2):277-86.
23. Zhang B, Chambers MC, Tabb DL. Proteomic parsimony through bipartite graph analysis improves accuracy and transparency. Journal of proteome research. 2007 Sep;6(9):3549-57.
24. Kim KY, Kim BJ, Yi GS. Reuse of imputed data in microarray analysis increases imputation efficiency. BMC Bioinformatics. 2004 Oct 26;5:160.

25. Benjamini Y HY. Controlling the false discovery rate: a practical and powerful approach to multiple testing. Journal of the Royal Statistical Society Series B. 1995;57:289-300.
26. Franz M, Lopes CT, Huck G, et al. Cytoscape.js: a graph theory library for visualisation and analysis. Bioinformatics. 2016 Jan 15;32(2):309-11.
27. Proto MC, Fiore D, Piscopo C, et al. Lipid homeostasis and mevalonate pathway in COVID-19: Basic concepts and potential therapeutic targets. Prog Lipid Res. 2021 Apr;82:101099.
28. Kumar L, M EF. Mfuzz: a software package for soft clustering of microarray data. Bioinformation. 2007 May 20;2(1):5-7.
29. Bi X, Liu W, Ding X, et al. Proteomic and metabolomic profiling of urine uncovers immune responses in patients with COVID-19. Cell Rep. 2022 Jan 18;38(3):110271.
30. Liu Y, Song L, Zheng N, et al. A urinary proteomic landscape of COVID-19 progression identifies signaling pathways and therapeutic options. Sci China Life Sci. 2022 Sep;65(9):1866-1880.
31. Liu T, Luo S, Libby P, et al. Cathepsin L-selective inhibitors: A potentially promising treatment for COVID-19 patients. Pharmacol Ther. 2020 Sep;213:107587.
32. Gomes CP, Fernandes DE, Casimiro F, et al. Cathepsin L in COVID-19: From Pharmacological Evidences to Genetics. Front Cell Infect Microbiol. 2020;10:589505.
33. Ou X, Liu Y, Lei X, et al. Characterization of spike glycoprotein of SARS-CoV-2 on virus entry and its immune cross-reactivity with SARS-CoV. Nat Commun. 2020 Mar 27;11(1):1620.
34. Hoffmann M, Kleine-Weber H, Schroeder S, et al. SARS-CoV-2 Cell Entry Depends on ACE2 and TMPRSS2 and Is Blocked by a Clinically Proven Protease Inhibitor. Cell. 2020 Apr 16;181(2):271-280.e8.
35. Katopodis P, Anikin V, Randeva HS, et al. Pan-cancer analysis of transmembrane protease serine 2 and cathepsin L that mediate cellular SARS-CoV-2 infection leading to COVID-19. Int J Oncol. 2020 Aug;57(2):533-539.
36. Thoms M, Buschauer R, Ameismeier M, et al. Structural basis for translational shutdown and immune evasion by the Nsp1 protein of SARS-CoV-2. Science. 2020 Sep 4;369(6508):1249-1255.
37. Schubert K, Karousis ED, Jomaa A, et al. SARS-CoV-2 Nsp1 binds the ribosomal mRNA channel to inhibit translation. Nat Struct Mol Biol. 2020 Oct;27(10):959-966.
38. Lapointe CP, Grosely R, Johnson AG, et al. Dynamic competition between SARS-CoV-2 NSP1 and mRNA on the human ribosome inhibits translation initiation. Proc Natl Acad Sci U S A. 2021 Feb 9;118(6).
39. Cauchois R, Koubi M, Delarbre D, et al. Early IL-1 receptor blockade in severe inflammatory respiratory failure complicating COVID-19. Proc Natl Acad Sci U S A. 2020 Aug 11;117(32):18951-18953.
40. Joshi MG, Kshersagar J, Desai SR, et al. Antiviral properties of placental growth factors: A novel therapeutic approach for COVID-19 treatment. Placenta. 2020 Sep 15;99:117-130.
41. Abers MS, Delmonte OM, Ricotta EE, et al. An immune-based biomarker signature is associated with mortality in COVID-19 patients. JCI Insight. 2021 Jan 11;6(1).

42. Satış H, Özger HS, Aysert Yıldız P, et al. Prognostic value of interleukin-18 and its association with other inflammatory markers and disease severity in COVID-19. Cytokine. 2021 Jan;137:155302.
43. Zhang C, Wu Z, Li JW, et al. Cytokine release syndrome in severe COVID-19: interleukin-6 receptor antagonist tocilizumab may be the key to reduce mortality. Int J Antimicrob Agents. 2020 May;55(5):105954.
44. Canziani LM, Trovati S, Brunetta E, et al. Interleukin-6 receptor blocking with intravenous tocilizumab in COVID-19 severe acute respiratory distress syndrome: A retrospective case-control survival analysis of 128 patients. J Autoimmun. 2020 Nov;114:102511.
45. Mojtabavi H, Saghazadeh A, Rezaei N. Interleukin-6 and severe COVID-19: a systematic review and meta-analysis. Eur Cytokine Netw. 2020 Jun 1;31(2):44-49.
46. Akgun E, Tuzuner MB, Sahin B, et al. Proteins associated with neutrophil degranulation are upregulated in nasopharyngeal swabs from SARS-CoV-2 patients. PLoS One. 2020;15(10):e0240012.
47. Cavalli G, Colafrancesco S, Emmi G, et al. Interleukin 1α: a comprehensive review on the role of IL-1α in the pathogenesis and treatment of autoimmune and inflammatory diseases. Autoimmun Rev. 2021 Mar;20(3):102763.
48. Han H, Ma Q, Li C, et al. Profiling serum cytokines in COVID-19 patients reveals IL-6 and IL-10 are disease severity predictors. Emerg Microbes Infect. 2020 Dec;9(1):1123-1130.
49. Chen Y, Wang J, Liu C, et al. IP-10 and MCP-1 as biomarkers associated with disease severity of COVID-19. Mol Med. 2020 Oct 29;26(1):97.
50. Yang Y, Shen C, Li J, et al. Plasma IP-10 and MCP-3 levels are highly associated with disease severity and predict the progression of COVID-19. J Allergy Clin Immunol. 2020 Jul;146(1):119-127.e4.
51. Vecchié A, Bonaventura A, Toldo S, et al. IL-18 and infections: Is there a role for targeted therapies? J Cell Physiol. 2021 Mar;236(3):1638-1657.
52. Tzouvelekis A, Ntolios P, Karameris A, et al. Increased expression of epidermal growth factor receptor (EGF-R) in patients with different forms of lung fibrosis. Biomed Res Int. 2013;2013:654354.
53. Venkataraman T, Frieman MB. The role of epidermal growth factor receptor (EGFR) signaling in SARS coronavirus-induced pulmonary fibrosis. Antiviral Res. 2017 Jul;143:142-150.
54. Qin X, Huang C, Wu K, et al. Anti-coronavirus disease 2019 (COVID-19) targets and mechanisms of puerarin. J Cell Mol Med. 2021 Jan;25(2):677-685.
55. Hidalgo A, Frenette PS. Leukocyte podosomes sense their way through the endothelium. Immunity. 2007 Jun;26(6):753-5.
56. Ueland T, Holter JC, Holten AR, et al. Distinct and early increase in circulating MMP-9 in COVID-19 patients with respiratory failure. J Infect. 2020 Sep;81(3):e41-e43.
57. Strieter RM, Mehrad B. New mechanisms of pulmonary fibrosis. Chest. 2009 Nov;136(5):1364-1370.
58. Fricke-Galindo I, Falfán-Valencia R. Genetics Insight for COVID-19 Susceptibility and Severity: A Review. Front Immunol. 2021;12:622176.
59. Young MJ, O'Hare M, Matiello M, et al. Creutzfeldt-Jakob disease in a man with COVID-19: SARS-CoV-2-accelerated neurodegeneration? Brain Behav Immun. 2020 Oct;89:601-603.

60. DeKosky ST, Kochanek PM, Valadka AB, et al. Blood Biomarkers for Detection of Brain Injury in COVID-19 Patients. J Neurotrauma. 2021 Jan 1;38(1):1-43.
61. Mao L, Jin H, Wang M, et al. Neurologic Manifestations of Hospitalized Patients With Coronavirus Disease 2019 in Wuhan, China. JAMA Neurol. 2020 Jun 1;77(6):683-690.
62. Li Z, Liu T, Yang N, et al. Neurological manifestations of patients with COVID-19: potential routes of SARS-CoV-2 neuroinvasion from the periphery to the brain. Front Med. 2020 Oct;14(5):533-541.
63. Chen T, Wu D, Chen H, et al. Clinical characteristics of 113 deceased patients with coronavirus disease 2019: retrospective study. Bmj. 2020 Mar 26;368:m1091.
64. Nath A. Neurologic complications of coronavirus infections. Neurology. 2020 May 12;94(19):809-810.
65. Troyer EA, Kohn JN, Hong S. Are we facing a crashing wave of neuropsychiatric sequelae of COVID-19? Neuropsychiatric symptoms and potential immunologic mechanisms. Brain Behav Immun. 2020 Jul;87:34-39.
66. Dubé M, Le Coupanec A, Wong AHM, et al. Axonal Transport Enables Neuron-to-Neuron Propagation of Human Coronavirus OC43. J Virol. 2018 Sep 1;92(17).
67. Wong SH, Lui RN, Sung JJ. Covid-19 and the digestive system. J Gastroenterol Hepatol. 2020 May;35(5):744-748.
68. Guidon AC, Amato AA. COVID-19 and neuromuscular disorders. Neurology. 2020 Jun 2;94(22):959-969.
69. Paliwal VK, Garg RK, Gupta A, et al. Neuromuscular presentations in patients with COVID-19. Neurol Sci. 2020 Nov;41(11):3039-3056.
70. García-Pérez BE, González-Rojas JA, Salazar MI, et al. Taming the Autophagy as a Strategy for Treating COVID-19. Cells. 2020 Dec 13;9(12).
71. Clemente V, D'Arcy P, Bazzaro M. Deubiquitinating Enzymes in Coronaviruses and Possible Therapeutic Opportunities for COVID-19. Int J Mol Sci. 2020 May 15;21(10).
72. Xiong Y, Liu Y, Cao L, et al. Transcriptomic characteristics of bronchoalveolar lavage fluid and peripheral blood mononuclear cells in COVID-19 patients. Emerg Microbes Infect. 2020 Dec;9(1):761-770.
73. Li S, Zhang Y, Guan Z, et al. SARS-CoV-2 triggers inflammatory responses and cell death through caspase-8 activation. Signal Transduct Target Ther. 2020 Oct 9;5(1):235.
74. Huang L, Shi Y, Gong B, et al. Dynamic blood single-cell immune responses in patients with COVID-19. Signal Transduct Target Ther. 2021 Mar 6;6(1):110.
75. Blasig IE, Haseloff RF. Tight junctions and tissue barriers. Antioxid Redox Signal. 2011 Sep 1;15(5):1163-6.
76. Sawada N. Tight junction-related human diseases. Pathol Int. 2013 Jan;63(1):1-12.
77. Wittekindt OH. Tight junctions in pulmonary epithelia during lung inflammation. Pflugers Arch. 2017 Jan;469(1):135-147.
78. Mazzon E, Cuzzocrea S. Role of TNF-alpha in lung tight junction alteration in mouse model of acute lung inflammation. Respir Res. 2007 Oct 30;8(1):75.
79. Serebrovska ZO, Chong EY, Serebrovska TV, et al. Hypoxia, HIF-1α, and COVID-19: from pathogenic factors to potential therapeutic targets. Acta Pharmacol Sin. 2020 Dec;41(12):1539-1546.
80. Nagao T. [Thrombolytic agents]. Nihon Rinsho. 2014 Jul;72(7):1254-7.

81. Hepner M, Karlaftis V. Antithrombin. Methods Mol Biol. 2013;992:355-64.
82. Ito T, Thachil J, Asakura H, et al. Thrombomodulin in disseminated intravascular coagulation and other critical conditions-a multi-faceted anticoagulant protein with therapeutic potential. Crit Care. 2019 Aug 15;23(1):280.
83. Marín-Corral J, Rodríguez-Morató J, Gomez-Gomez A, et al. Metabolic Signatures Associated with Severity in Hospitalized COVID-19 Patients. Int J Mol Sci. 2021 Apr 30;22(9).
84. Zhang Y, Lin F, Tu W, et al. Thyroid dysfunction may be associated with poor outcomes in patients with COVID-19. Mol Cell Endocrinol. 2021 Feb 5;521:111097.
85. Smith SM, Boppana A, Traupman JA, et al. Impaired glucose metabolism in patients with diabetes, prediabetes, and obesity is associated with severe COVID-19. J Med Virol. 2021 Jan;93(1):409-415.
86. Vassiliou AG, Athanasiou N, Keskinidou C, et al. Increased Glucocorticoid Receptor Alpha Expression and Signaling in Critically Ill Coronavirus Disease 2019 Patients. Crit Care Med. 2021 May 25.
87. Beale DJ, Shah R, Karpe AV, et al. Metabolic Profiling from an Asymptomatic Ferret Model of SARS-CoV-2 Infection. Metabolites. 2021 May 19;11(5).

Figure Legends

Figure 1. Timeline of the disease course and sample acquisition of COVID-19 patients, including 12 mild patients, 16 severe patients and two fatal patients. Further details are presented in Table 1 and Table S1.

Figure 2. Quality control of proteomic data and the correlation with clinical indicators. (A) t-distributed stochastic neighbor embedding (t-SNE) of urine samples using 2574 measured urine protein groups. (B). Pearson correlation analysis between the differentially expressed proteins in the onset period and 28 clinical indicators.

Figure 3. Viral infection and immune response changes in COVID-19 patients in the onset and recovery periods.

(A). The dysregulated pathways and disease/biofunctions associated with viral infections. Pathway and disease/biofunction enrichment analyses were performed using differential proteins in the six phases (M, S, F, MRE, SRE, and SRT) using IPA. The size of the circle represents the -log10(p value), and the color represents the Z score by IPA.

(B). Heatmap of 21 differentially expressed proteins associated with the coronavirus replication pathway and the coronavirus pathogenesis pathway. The average abundance of proteins in the six phases of COVID-19 was calculated and visualized as a heatmap.

(C). Protein expression of ACE2, TMPRSS2 and CTSL in the six phases (M, S, F, MRE, SRE, and SRT) of COVID-19 and healthy controls. The y-axis represents the protein expression transformed by the log2 abundance. Pairwise comparison of each protein between the six phases and the healthy control was performed with Student's t test. The cutoff of the significant phase was set at a B-H adjusted p value<0.05 and FC>2 or <0.5. B-H adjusted p value: *p<0.05; **p<0.01; ***p<0.001.

(D). The dysregulated pathways associated with immune response changes. Pathway enrichment analysis was performed using differential proteins in the six phases (M, S, F, MRE, SRE, and SRT) using IPA. The color represents the -log10(p value) by IPA.

(E). Heatmap of the immune response classified into seven clusters using the ImmPort database. The average abundance of proteins in the six phases of COVID-19 was calculated and visualized as a heatmap.

(F). Clinical parameters and the protein expression levels of EGF and IL-18 in the active and recovery periods of COVID-19 patients. The y-axis represents the protein expression transformed by the log2 abundance or the concentration in serum. The significance indicated by the asterisks. For the clinical parameters, the unpaired two-sided Welch's t test was performed (p value: *, < 0.05; **, < 0.01; ***, < 0.001). For urine protein expression levels, significance was set at B-H adjusted p value<0.05 and FC>2 or <0.5. B-H adjusted p value: *p<0.05; **p<0.01; ***p<0.001.

Figure 4. Multiple organ damage, cell injury, coagulation system changes and metabolic changes in COVID-19 patients in the onset and recovery periods.

(A). Heatmap of common differential urine proteins identified in the autopsy results of the heart, kidney, lung and liver. The average abundance of proteins in the six phases of COVID-19 was calculated and visualized as a heatmap.

(B). The dysregulated pathways and disease/biofunctions associated with neurological system changes. Pathway and disease/biofunction enrichment analyses were performed using differential proteins in the six phases (M, S, F, MRE, SRE, and SRT) using IPA. The color represents the -log10(p value) by IPA.
(C). The dysregulated pathways associated with coagulation system changes. Pathway enrichment analysis was performed using differential proteins in the six phases (M, S, F, MRE, SRE, and SRT) using IPA. The color represents the -log10(p value) by IPA.
(D). Heatmap of 18 differentially expressed proteins associated with the coagulation system. The average abundance of proteins in the six phases of COVID-19 was calculated and visualized as a heatmap.
(E). The dysregulated pathways associated with cell injury. Pathway enrichment analysis was performed using differential proteins in the six phases (M, S, F, MRE, SRE, and SRT) using IPA. The size of the circle represents the -log10(p value), and the color represents the Z score by IPA.
(F). The dysregulated pathways associated with metabolic changes. Pathway enrichment analysis was performed using differential proteins in the six phases (M, S, F, MRE, SRE, and SRT) using IPA. The size of the circle represents the -log10(p value), and the color represents the Z score by IPA.

Figure 5. Potential monitoring biomarkers in the COVID-19 active and recovery periods.

(A). Identification of specific clusters in COVID-19 patients. A total of 1181 differentially expressed proteins in the COVID-19 active period were clustered using mFuzz into significant discrete clusters to illustrate the relative expression changes of the 1186 differentially expressed proteins. The groups in proteomics data: 1: Healthy; 2: Mild; 3: Severe; 4: Fatal; 5: MRE; 6: SRE; 7: SRT.
(B). Protein expression of CFB, SOD1, EGF and KNG1 in the six phases (M, S, F, MRE, SRE, and SRT) of COVID-19 and healthy controls. The y-axis represents the protein expression transformed by the log2 abundance. Pairwise comparison of each protein between the six phases and the healthy control was performed with Student's t test. The cutoff of the significant phase was set at a B-H adjusted p value<0.05 and FC>2 or <0.5. B-H adjusted p value: *p<0.05; **p<0.01; ***p<0.001.
(C). Validation of CFB, SOD1, EGF and KNG1 expression in 10 COVID-19 patients, including 4 mild and 6 severe patients. The y-axis represents the protein expression transformed by the log2 abundance.
(D). The ten hub proteins of differential proteins in the mild, severe and fatal phases using the MCC method in the cytoHubba module of CytoScape.

Figure 6. Dysregulated proteins and pathways in six aspects of functional changes in COVID-19. A hypothetical system view of multiple functional changes in response to SARS-CoV-2 infection. Red boxes: upregulated proteins; green boxes: downregulated proteins; orange/pink box: molecular processes; white box: related immune cells.

Table 1. Demographics and baseline characteristics of COVID-19 patients in their active and recovery periods.

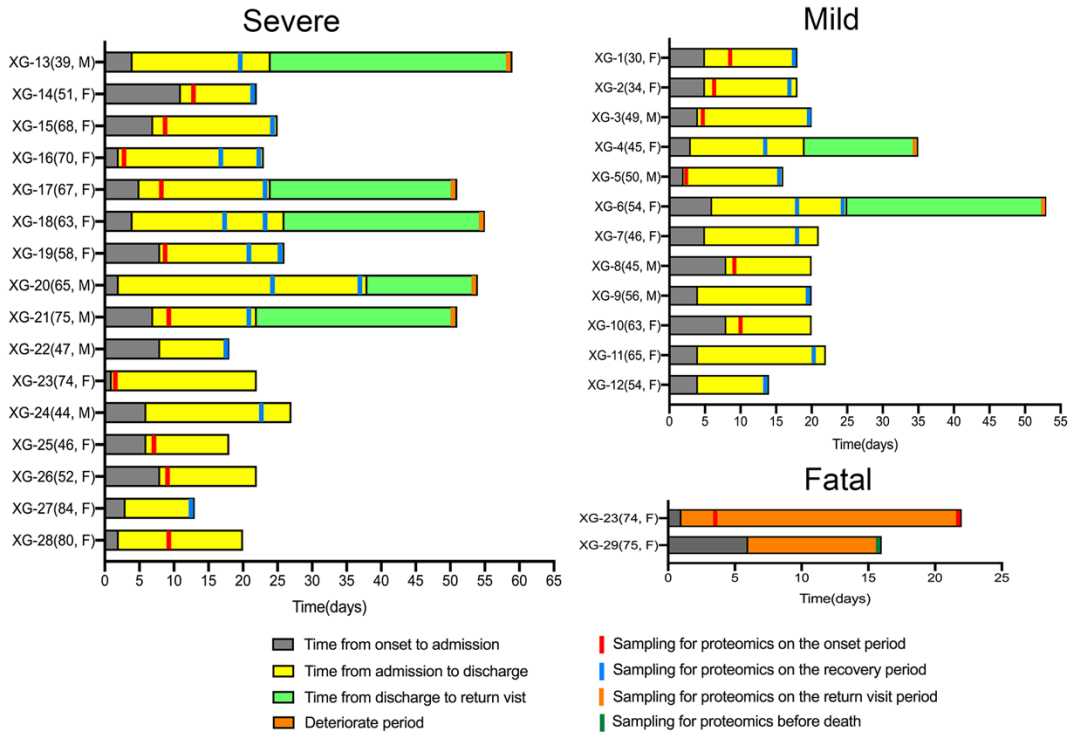

Figure 1. Timeline of the disease course and sample acquisition of COVID-19 patients, including 12 mild patients, 16 severe patients and two fatal patients. Further details are presented in Table 1 and Table S1.

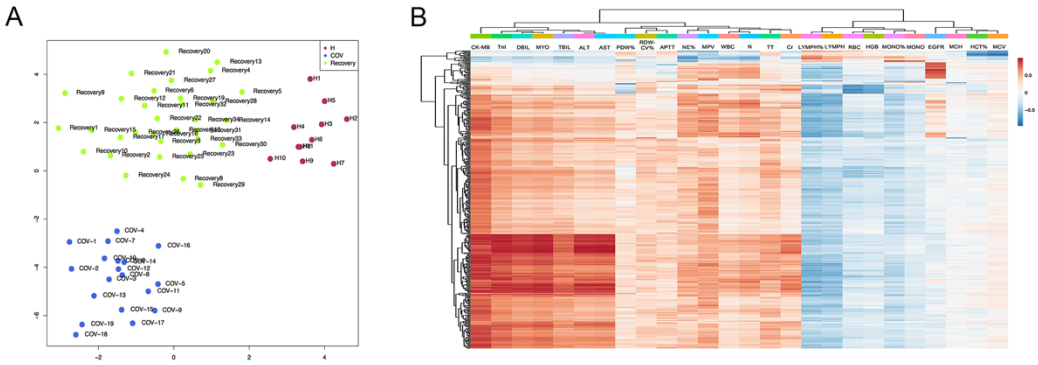

Figure 2. Quality control of proteomic data and the correlation with clinical indicators. (A) t-distributed stochastic neighbor embedding (t-SNE) of urine samples using 2574 measured urine protein groups. (B). Pearson correlation analysis between the differentially expressed proteins in the onset period and 28 clinical indicators.

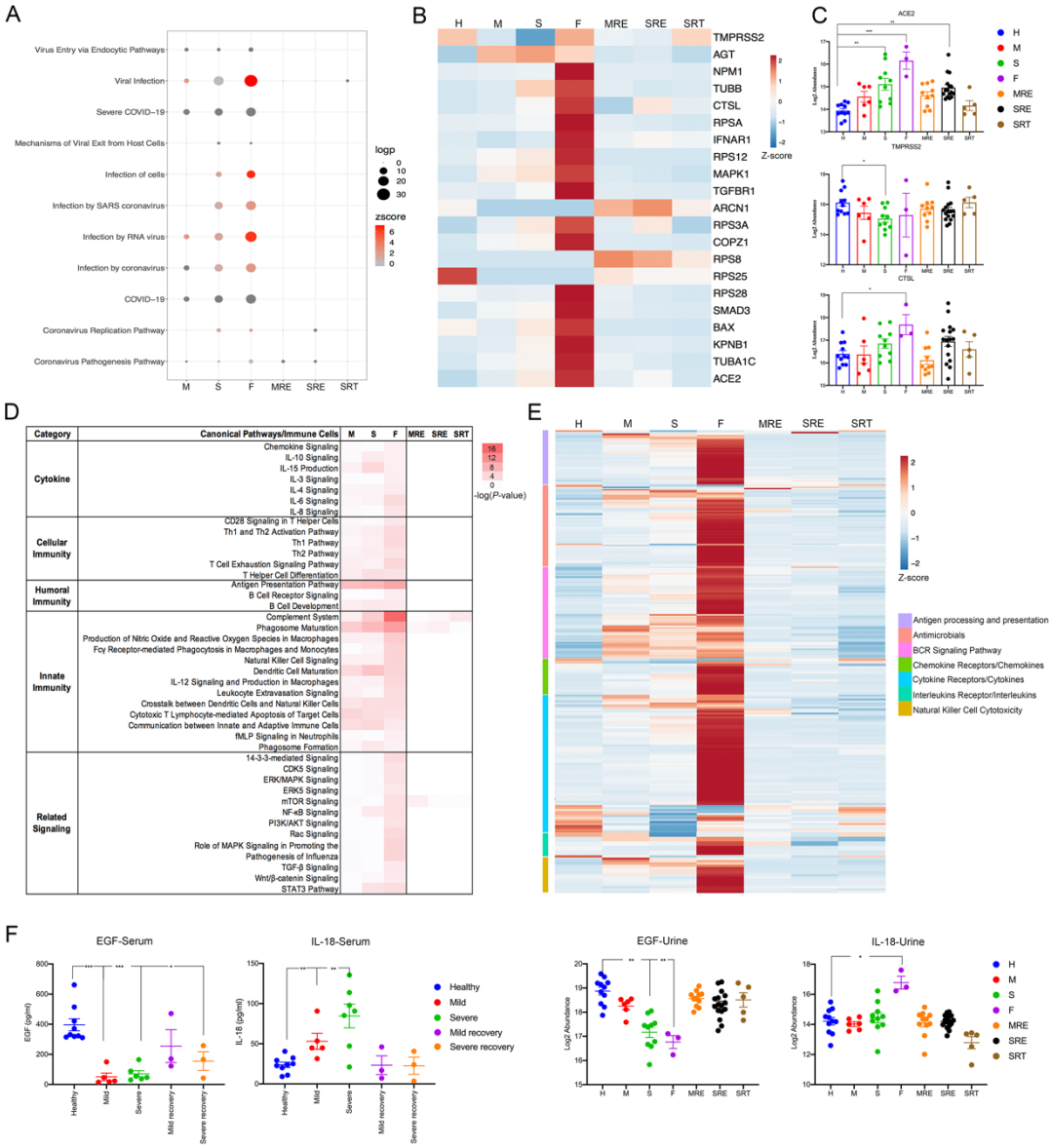

Figure 3. Viral infection and immune response changes in COVID-19 patients in the onset and recovery periods.

(A). The dysregulated pathways and disease/biofunctions associated with viral infections. Pathway and disease/biofunction enrichment analyses were performed using differential proteins in the six phases (M, S, F, MRE, SRE, and SRT) using IPA. The size of the circle represents the -log10(p value), and the color represents the Z score by IPA.

(B). Heatmap of 21 differentially expressed proteins associated with the coronavirus replication pathway and the coronavirus pathogenesis pathway. The average abundance of proteins in the six phases of COVID-19 was calculated and visualized as a heatmap.

(C). Protein expression of ACE2, TMPRSS2 and CTSL in the six phases (M, S, F, MRE, SRE, and SRT) of COVID-19 and healthy controls. The y-axis represents the protein expression transformed by the log2 abundance. Pairwise comparison of each

protein between the six phases and the healthy control was performed with Student's t test. The cutoff of the significant phase was set at a B-H adjusted p value<0.05 and FC>2 or <0.5. B-H adjusted p value: *p<0.05; **p<0.01; ***p<0.001.
(D). The dysregulated pathways associated with immune response changes. Pathway enrichment analysis was performed using differential proteins in the six phases (M, S, F, MRE, SRE, and SRT) using IPA. The color represents the -log10(p value) by IPA.
(E). Heatmap of the immune response classified into seven clusters using the ImmPort database. The average abundance of proteins in the six phases of COVID-19 was calculated and visualized as a heatmap.
(F). Clinical parameters and the protein expression levels of EGF and IL-18 in the active and recovery periods of COVID-19 patients. The y-axis represents the protein expression transformed by the log2 abundance or the concentration in serum. The significance indicated by the asterisks. For the clinical parameters, the unpaired two-sided Welch's t test was performed (p value: *, < 0.05; **, < 0.01; ***, < 0.001). For urine protein expression levels, significance was set at B-H adjusted p value<0.05 and FC>2 or <0.5. B-H adjusted p value: *p<0.05; **p<0.01; ***p<0.001.

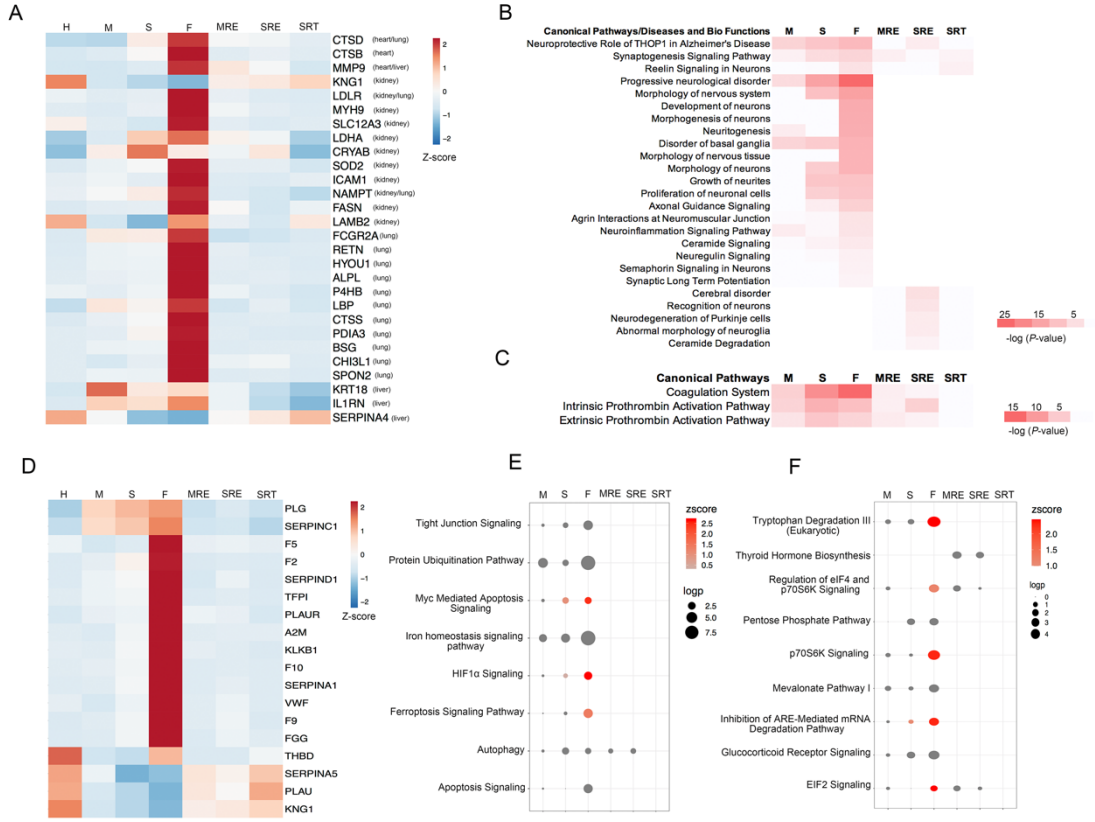

Figure 4. Multiple organ damage, cell injury, coagulation system changes and metabolic changes in COVID-19 patients in the onset and recovery periods.

(A). Heatmap of common differential urine proteins identified in the autopsy results of the heart, kidney, lung and liver. The average abundance of proteins in the six phases of COVID-19 was calculated and visualized as a heatmap.

(B). The dysregulated pathways and disease/biofunctions associated with neurological system changes. Pathway and disease/biofunction enrichment analyses were performed using differential proteins in the six phases (M, S, F, MRE, SRE, and SRT) using IPA. The color represents the -log10(p value) by IPA.

(C). The dysregulated pathways associated with coagulation system changes. Pathway enrichment analysis was performed using differential proteins in the six phases (M, S, F, MRE, SRE, and SRT) using IPA. The color represents the -log10(p value) by IPA.

(D). Heatmap of 18 differentially expressed proteins associated with the coagulation system. The average abundance of proteins in the six phases of COVID-19 was calculated and visualized as a heatmap.

(E). The dysregulated pathways associated with cell injury. Pathway enrichment analysis was performed using differential proteins in the six phases (M, S, F, MRE, SRE, and SRT) using IPA. The size of the circle represents the -log10(p value), and the color represents the Z score by IPA.

(F). The dysregulated pathways associated with metabolic changes. Pathway enrichment analysis was performed using differential proteins in the six phases (M, S, F, MRE, SRE, and SRT) using IPA. The size of the circle represents the -log10(p value), and the color represents the Z score by IPA.

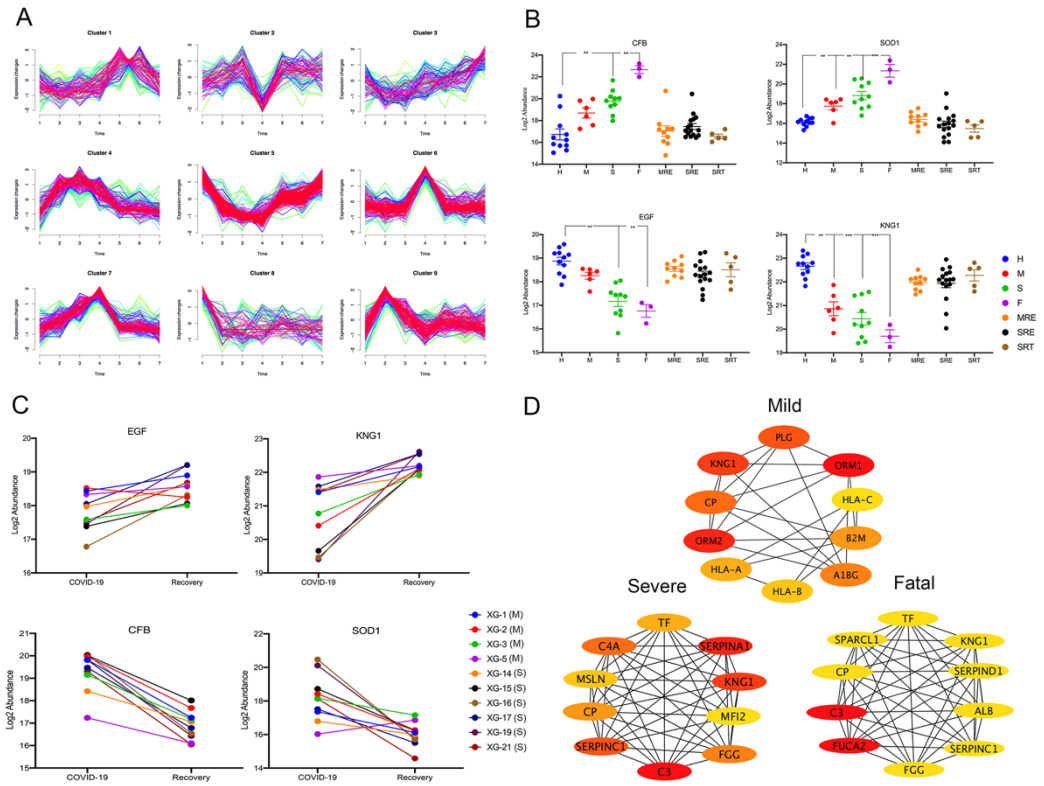

Figure 5. Potential monitoring biomarkers in the COVID-19 active and recovery periods.

(A). Identification of specific clusters in COVID-19 patients. A total of 1181 differentially expressed proteins in the COVID-19 active period were clustered using mFuzz into significant discrete clusters to illustrate the relative expression changes of the 1186 differentially expressed proteins. The groups in proteomics data: 1: Healthy; 2: Mild; 3: Severe; 4: Fatal; 5: MRE; 6: SRE; 7: SRT.

(B). Protein expression of CFB, SOD1, EGF and KNG1 in the six phases (M, S, F, MRE, SRE, and SRT) of COVID-19 and healthy controls. The y-axis represents the protein expression transformed by the log2 abundance. Pairwise comparison of each protein between the six phases and the healthy control was performed with Student's t test. The cutoff of the significant phase was set at a B-H adjusted p value<0.05 and FC>2 or <0.5. B-H adjusted p value: *p<0.05; **p<0.01; ***p<0.001.

(C). Validation of CFB, SOD1, EGF and KNG1 expression in 10 COVID-19 patients, including 4 mild and 6 severe patients. The y-axis represents the protein expression transformed by the log2 abundance.

(D). The ten hub proteins of differential proteins in the mild, severe and fatal phases using the MCC method in the cytoHubba module of CytoScape.

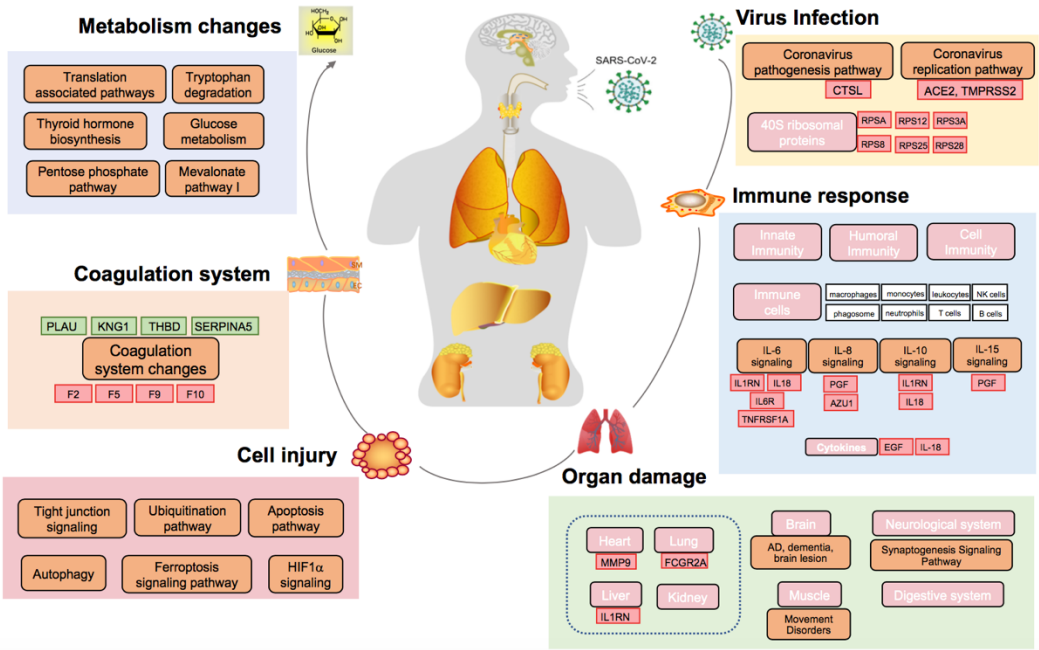

Figure 6. Dysregulated proteins and pathways in six aspects of functional changes in COVID-19. A hypothetical system view of multiple functional changes in response to SARS-CoV-2 infection. Red boxes: upregulated proteins; green boxes: downregulated proteins; orange/pink box: molecular processes; white box: related immune cells.

Table1. Demographics and baseline characteristics of COVID-19 patients in their active and recovery period.

Variables	Healthy Control (n=11)	COVID-19 patients (n=29)			Recovery patients (n= 27)			
		Mild (n=12)	Severe (n=16)	Fatal (n=2)	Mild Remission (n=12)	Mild Return Visit (n=2）	Severe Remission (n=15)	Severe Return Visit (n=5)
Sex - no. (%)								
Male	5 (45.5)	4 (33.3)	7 (43.8)	0 (0.00)	4 (33.3)	0（0.0）	7(46.7)	3(60.0)
Female	6 (54.5)	8 (66.7)	9 (56.2)	2 (100.0)	8 (66.7)	2(100.0)	8(53.3)	2(40.0)
Age - year								
Mean ± SD	42.9±6.5	49.3±10.3	61.4±13.7	74.5±0.7	49.3±10.3	49.5±6.4	60.6±13.8	61.8±13.5
Median (IQR)	42.0（38.0-46.0）	49.0（45.0-56.0）	64.0（48.0-73.0）	——	49.5（45.25-55.5）	——	63.0（47.0-70.0）	65.0（51.0-71.0）
Range	34-56	30-65	39-84	74.0-75.0	30-65	45-54	39-84	39-75
Smoke - no. (%)		1(8.3)	1(6.2)	0（0.0）	1(8.3)	0(0.0)	1(6.7)	0(0.0)
Alcohol - no. (%)		0(0.0)	1(6.2)	0（0.0）	0(0.0)	0(0.0)	1(6.7)	0(0.0)
Time from Onset to Admission, Days								
Mean ± SD		4.8±1.3	5.3±2.8	3.5±3.5				
Median (IQR)		4.5（4.0-5.75）	5.5（2.25-7.75）	——				
Range		2.0-8.0	1.0-11.0	1.0-6.0				
Time from Admission to Severe, Days								
Mean ± SD			2.8±3.0					
Median (IQR)			2.0（0.0-4.75）					
Range			0.0-9.0					
Symptoms - no. (%)								
Fever		10(83.3)	16(100.0)	2(100.0)	0(0.0)		0(0.0)	
Cough		10(83.3)	12(75.0)	1(50.0)	7(58.3)		8(53.3)	
Headache		2(16.7)	2(12.5)	0(0.0)	0(0.0)		0(0.0)	
Fatigue		3(25.0)	11(68.8)	2(100.0)	0(0.0)		4(26.7)	
Shortness of breath		1(8.3)	9(56.3)	2(100.0)	1(8.3)		4(26.7)	
Nausea or vomiting		2(16.7)	4(25.0)	0(0.0)	0(0.0)		2(13.3)	

Expectoration	8(66.7)	6(37.5)	1(50.0)	3(25.0)		3(20.0)	
Diarrhea	1(8.3)	2(12.5)	2(100.0)	0(0.0)		1(6.7)	
Chest tightness	1(8.3)	8(50.0)	2(100.0)	0(0.0)		3(20.0)	
Chest CT - no. (%)							
Involvement of chest radiographs	11(91.7)	16(100.0)	2(100.0)	11(91.7)		15(100.0)	
Comorbidity- no. (%)							
Hypertension	1(8.3)	6(37.5)	2(100.0)	1(8.3)	0(0.0)	5(33.3)	1(20.0)
Diabetes	1(8.3)	1(6.3)	0(0.0)	1(8.3)	0(0.0)	1(6.7)	0(0.0)
Respiratory system	0(0.0)	1(6.3)	0(0.0)	0(0.0)	0(0.0)	1(6.7)	0(0.0)
Other Endocrine system	0(0.0)	1(6.3)	0(0.0)	0(0.0)	0(0.0)	1(6.7)	0(0.0)
Heart disease	0(0.0)	1(6.3)	1(50.0)	0(0.0)	0(0.0)	1(6.7)	1(20.0)
Digestive system	2(16.7)	1(6.3)	0(0.0)	2(16.7)	0(0.0)	1(6.7)	1(20.0)
Treatment - no. (%)							
Oxygen inhalation	3(25.0)	16(100.0)	2(100.0)	1(8.3)		13(86.7)	
Antibiotics	0(0.0)	5(31.3)	2(100.0)	0(0.0)		2(13.3)	
Antiviral drug	1(8.3)	6(37.5)	2(100.0)	0(0.0)		3(20.0)	
Immunoglobulin	0(0.0)	1(6.3)	0(0.0)	0(0.0)		1(6.7)	
Methylprednisolone	1(8.3)	11(68.8)	2(100.0)	1(8.3)		8(53.3)	
Chloroquine phosphate	5(41.7)	2(12.5)	0(0.0)	5(41.7)		0(0.0)	
Chinese medicine	11(91.7)	15(93.8)	2(100.0)	11(91.7)		14(93.3)	

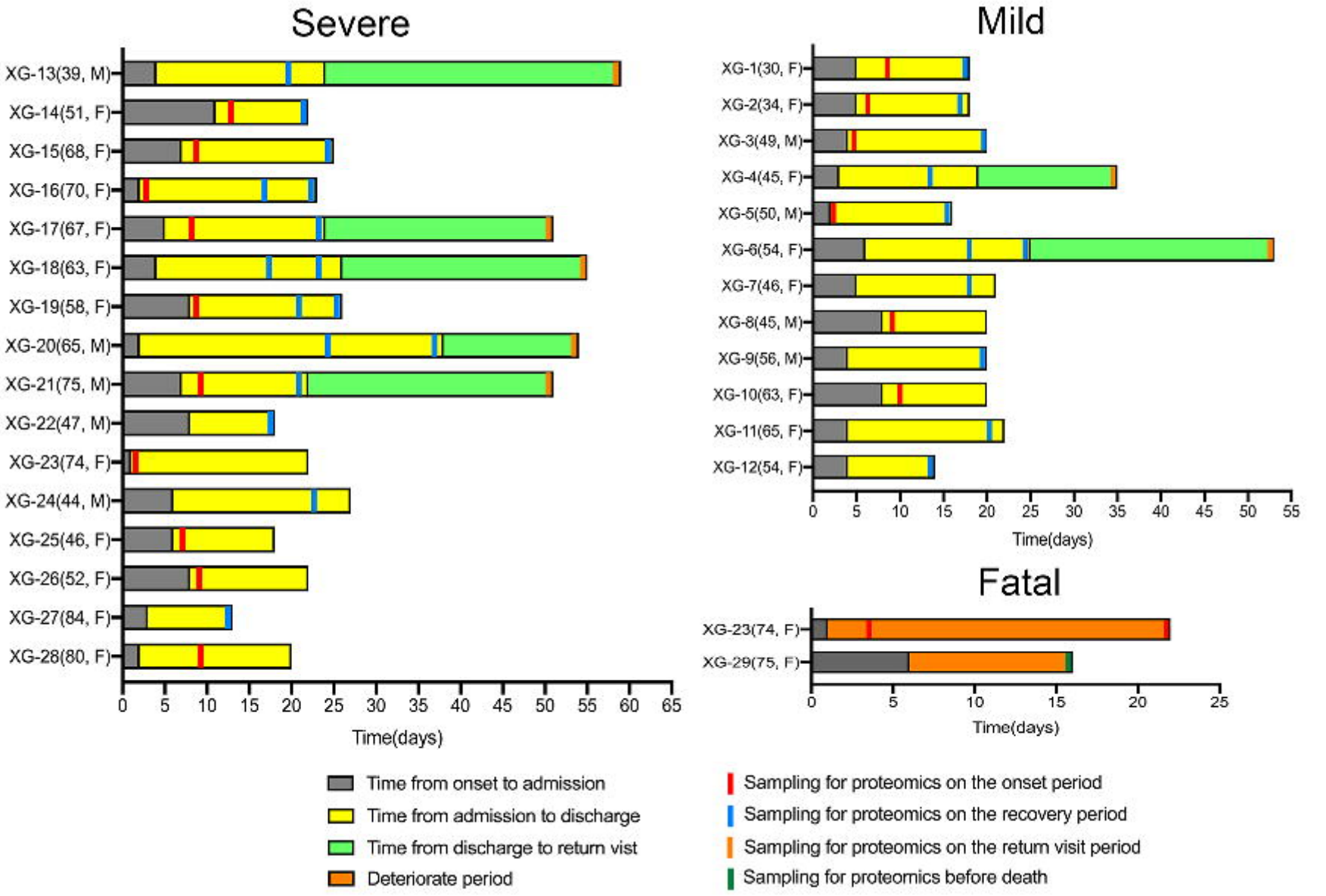
Severe
XG-13(39, M)
XG-14(51, F)
XG-15(68, F)
XG-16(70, F)
XG-17(67, F)
XG-18(63, F)
XG-19(58, F)
XG-20(65, M)
XG-21(75, M)
XG-22(47, M)
XG-23(74, F)
XG-24(44, M)
XG-25(46, F)
XG-26(52, F)
XG-27(84, F)
XG-28(80, F)
0 5 10 15 20 25 30 35 40 45 50 55 60 65
Time(days)
Mild
XG-1(30, F)
XG-2(34, F)
XG-3(49, M)
XG-4(45, F)
XG-5(50, M)
XG-6(54, F)
XG-7(46, F)
XG-8(45, M)
XG-9(56, M)
XG-10(63, F)
XG-11(65, F)
XG-12(54, F)
0 5 10 15 20 25 30 35 40 45 50 55
Time(days)
Fatal
XG-23(74, F)
XG-29(75, F)
0 5 10 15 20 25
Time(days)
Time from onset to admission
Time from admission to discharge
Time from discharge to return vist
Deteriorate period
Sampling for proteomics on the onset period
Sampling for proteomics on the recovery period
Sampling for proteomics on the return visit period
Sampling for proteomics before death

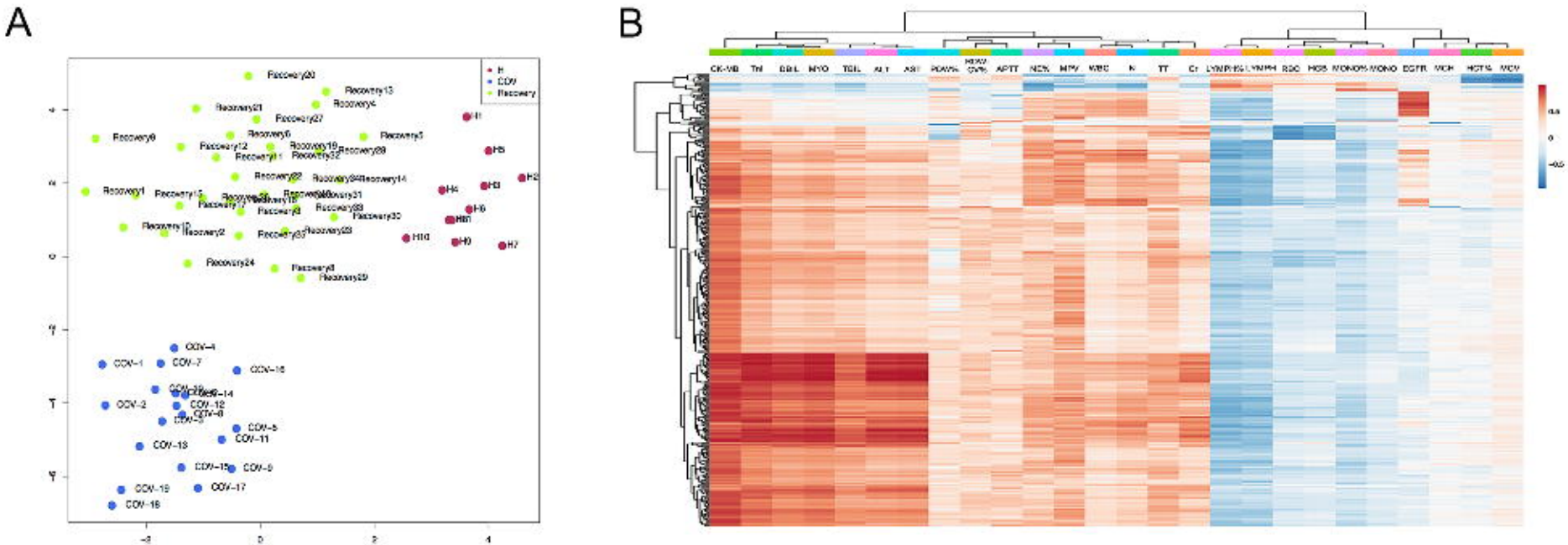
A
B
H
COV
Recovery

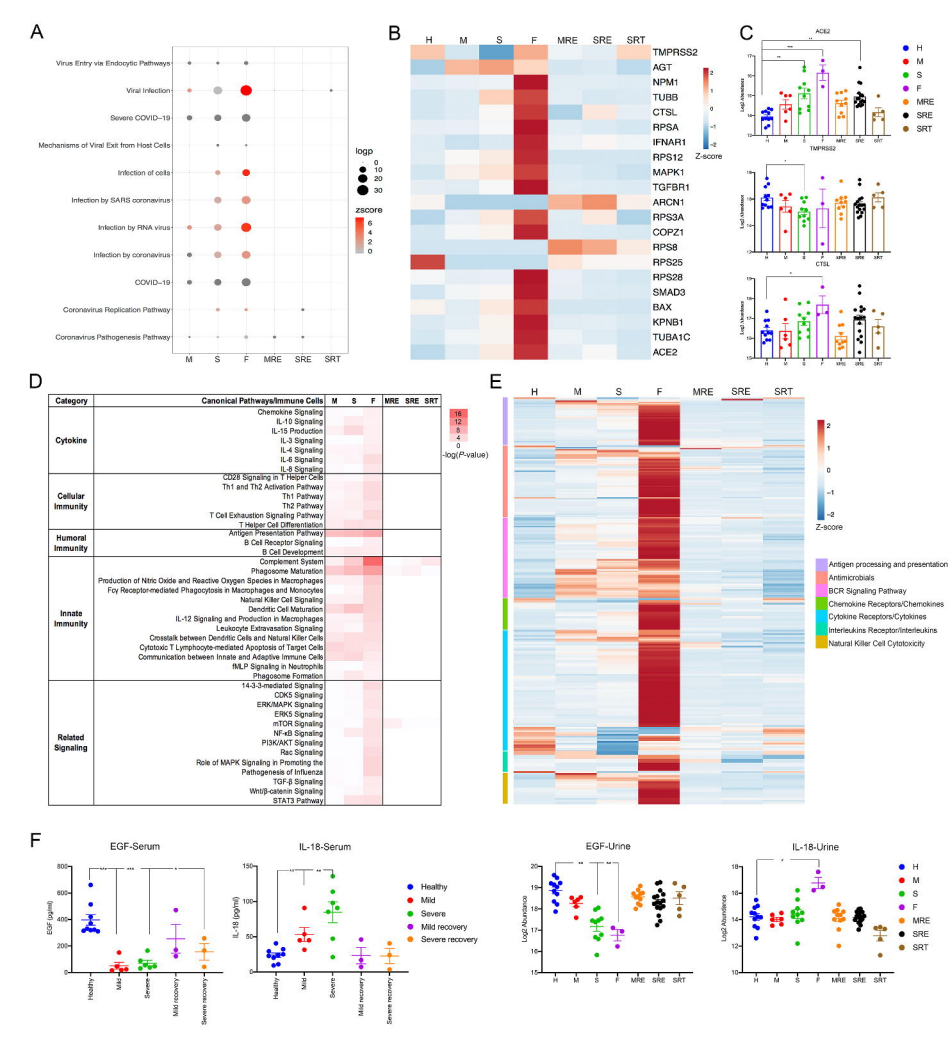
A
Virus Entry via Endocytic Pathways
Viral Infection
Severe COVID-19
Mechanisms of Viral Exit from Host Cells
Infection of cells
Infection by SARS coronavirus
Infection by RNA virus
Infection by coronavirus
COVID-19
Coronavirus Replication Pathway
Coronavirus Pathogenesis Pathway
M S F MRE SRE SRT
logp
zscore
B
H M S F MRE SRE SRT
TMPRSS2
AGT
NPM1
TUBB
CTSL
RPSA
IFNAR1
RPS12
MAPK1
TGFBR1
ARCN1
RPS3A
COPZ1
RPS8
RPS25
RPS28
SMAD3
BAX
KPNB1
TUBA1C
ACE2
Z-score
C
ACE2
TMPRSS2
CTSL
Log2 Abundance
H M S F MRE SRE SRT
D
Category
Canonical Pathways/Immune Cells
M S F MRE SRE SRT
Cytokine
Chemokine Signaling
IL-10 Signaling
IL-15 Production
IL-3 Signaling
IL-4 Signaling
IL-6 Signaling
IL-8 Signaling
Cellular Immunity
CD28 Signaling in T Helper Cells
Th1 and Th2 Activation Pathway
Th1 Pathway
Th2 Pathway
T Cell Exhaustion Signaling Pathway
T Helper Cell Differentiation
Humoral Immunity
Antigen Presentation Pathway
B Cell Receptor Signaling
B Cell Development
Innate Immunity
Complement System
Phagosome Maturation
Production of Nitric Oxide and Reactive Oxygen Species in Macrophages
Fcγ Receptor-mediated Phagocytosis in Macrophages and Monocytes
Natural Killer Cell Signaling
Dendritic Cell Maturation
IL-12 Signaling and Production in Macrophages
Leukocyte Extravasation Signaling
Crosstalk between Dendritic Cells and Natural Killer Cells
Cytotoxic T Lymphocyte-mediated Apoptosis of Target Cells
Communication between Innate and Adaptive Immune Cells
fMLP Signaling in Neutrophils
Phagosome Formation
Related Signaling
14-3-3-mediated Signaling
CDK5 Signaling
ERK/MAPK Signaling
ERK5 Signaling
mTOR Signaling
NF-κB Signaling
PI3K/AKT Signaling
Rac Signaling
Role of MAPK Signaling in Promoting the Pathogenesis of Influenza
TGF-β Signaling
Wnt/β-catenin Signaling
STAT3 Pathway
-log(P-value)
E
H M S F MRE SRE SRT
Z-score
Antigen processing and presentation
Antimicrobials
BCR Signaling Pathway
Chemokine Receptors/Chemokines
Cytokine Receptors/Cytokines
Interleukins Receptor/Interleukins
Natural Killer Cell Cytotoxicity
F
EGF-Serum
IL-18-Serum
EGF-Urine
IL-18-Urine
EGF (pg/ml)
IL-18 (pg/ml)
Log2 Abundance
Healthy
Mild
Severe
Mild recovery
Severe recovery
H M S F MRE SRE SRT

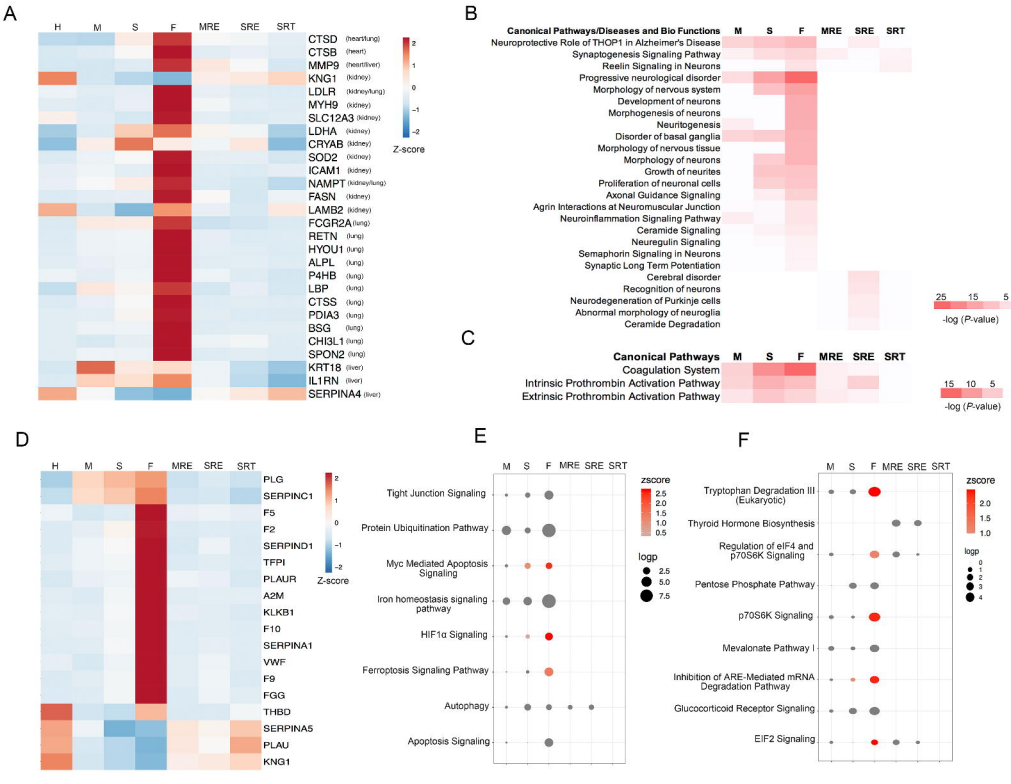
A
H M S F MRE SRE SRT
CTSD (heart/lung)
CTSB (heart)
MMP9 (heart/liver)
KNG1 (kidney)
LDLR (kidney/lung)
MYH9 (kidney)
SLC12A3 (kidney)
LDHA (kidney)
CRYAB (kidney)
SOD2 (kidney)
ICAM1 (kidney)
NAMPT (kidney/lung)
FASN (kidney)
LAMB2 (kidney)
FCGR2A (lung)
RETN (lung)
HYOU1 (lung)
ALPL (lung)
P4HB (lung)
LBP (lung)
CTSS (lung)
PDIA3 (lung)
BSG (lung)
CHI3L1 (lung)
SPON2 (lung)
KRT18 (liver)
IL1RN (liver)
SERPINA4 (liver)
2 1 0 −1 −2
Z-score
B
Canonical Pathways/Diseases and Bio Functions M S F MRE SRE SRT
Neuroprotective Role of THOP1 in Alzheimer's Disease
Synaptogenesis Signaling Pathway
Reelin Signaling in Neurons
Progressive neurological disorder
Morphology of nervous system
Development of neurons
Morphogenesis of neurons
Neuritogenesis
Disorder of basal ganglia
Morphology of nervous tissue
Morphology of neurons
Growth of neurites
Proliferation of neuronal cells
Axonal Guidance Signaling
Agrin Interactions at Neuromuscular Junction
Neuroinflammation Signaling Pathway
Ceramide Signaling
Neuregulin Signaling
Semaphorin Signaling in Neurons
Synaptic Long Term Potentiation
Cerebral disorder
Recognition of neurons
Neurodegeneration of Purkinje cells
Abnormal morphology of neuroglia
Ceramide Degradation
25 15 5
-log (P-value)
C
Canonical Pathways M S F MRE SRE SRT
Coagulation System
Intrinsic Prothrombin Activation Pathway
Extrinsic Prothrombin Activation Pathway
15 10 5
-log (P-value)
D
H M S F MRE SRE SRT
PLG
SERPINC1
F5
F2
SERPIND1
TFPI
PLAUR
A2M
KLKB1
F10
SERPINA1
VWF
F9
FGG
THBD
SERPINA5
PLAU
KNG1
2 1 0 −1 −2
Z-score
E
M S F MRE SRE SRT
Tight Junction Signaling
Protein Ubiquitination Pathway
Myc Mediated Apoptosis Signaling
Iron homeostasis signaling pathway
HIF1α Signaling
Ferroptosis Signaling Pathway
Autophagy
Apoptosis Signaling
zscore
2.5 2.0 1.5 1.0 0.5
logp
2.5 5.0 7.5
F
M S F MRE SRE SRT
Tryptophan Degradation III (Eukaryotic)
Thyroid Hormone Biosynthesis
Regulation of eIF4 and p70S6K Signaling
Pentose Phosphate Pathway
p70S6K Signaling
Mevalonate Pathway I
Inhibition of ARE-Mediated mRNA Degradation Pathway
Glucocorticoid Receptor Signaling
EIF2 Signaling
zscore
2.0 1.5 1.0
logp
0 1 2 3 4

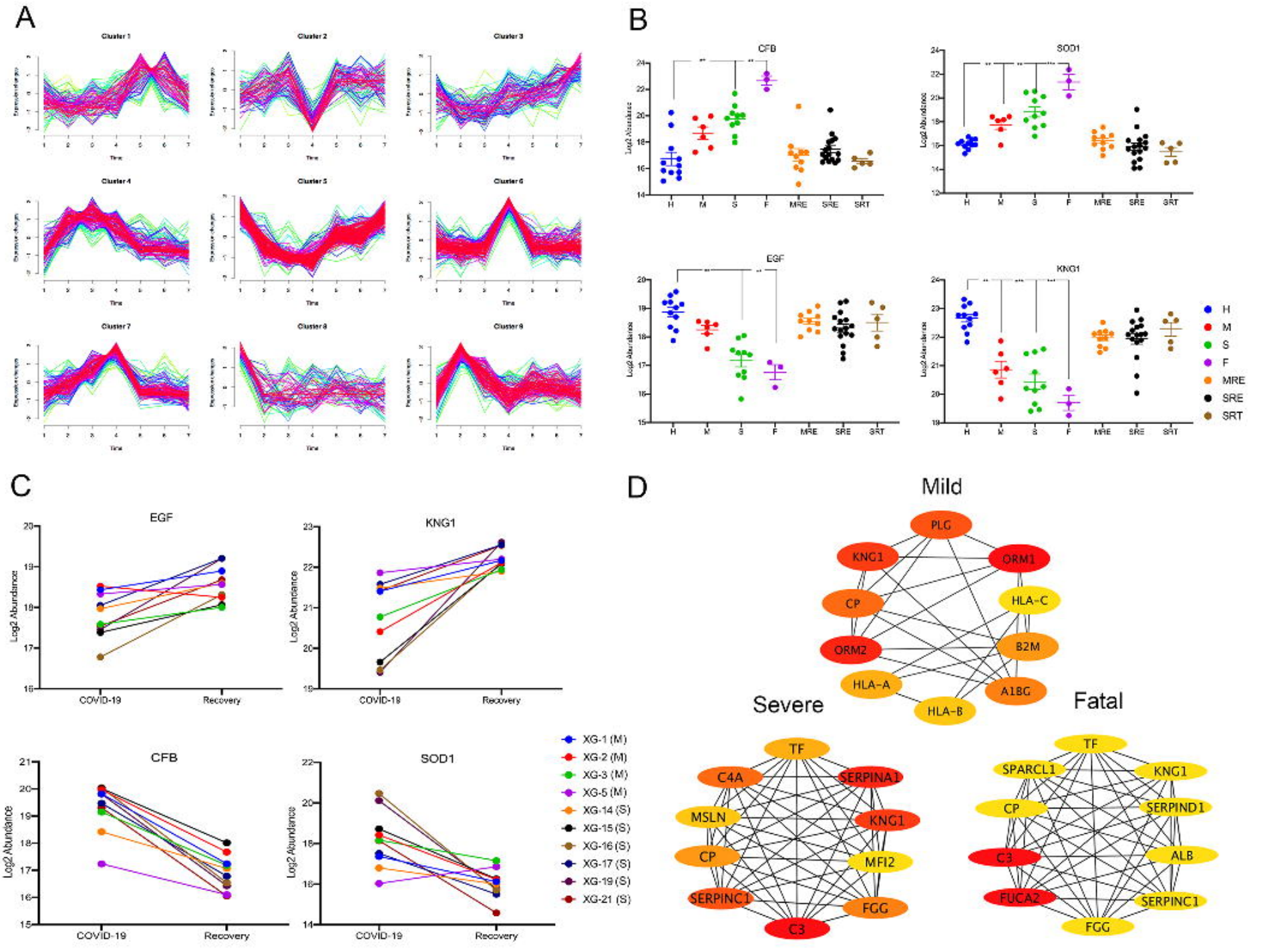
A
Cluster 1
Cluster 2
Cluster 3
Cluster 4
Cluster 5
Cluster 6
Cluster 7
Cluster 8
Cluster 9
Time
B
CFB
SOD1
EGF
KNG1
Log2 Abundance
H
M
S
F
MRE
SRE
SRT
C
EGF
KNG1
CFB
SOD1
Log2 Abundance
COVID-19
Recovery
XG-1 (M)
XG-2 (M)
XG-3 (M)
XG-5 (M)
XG-14 (S)
XG-15 (S)
XG-16 (S)
XG-17 (S)
XG-19 (S)
XG-21 (S)
D
Mild
PLG
KNG1
ORM1
CP
HLA-C
ORM2
B2M
HLA-A
A1BG
HLA-B
Severe
TF
C4A
SERPINA1
MSLN
KNG1
CP
MFI2
SERPINC1
FGG
C3
Fatal
TF
SPARCL1
KNG1
CP
SERPIND1
C3
ALB
FUCA2
SERPINC1
FGG

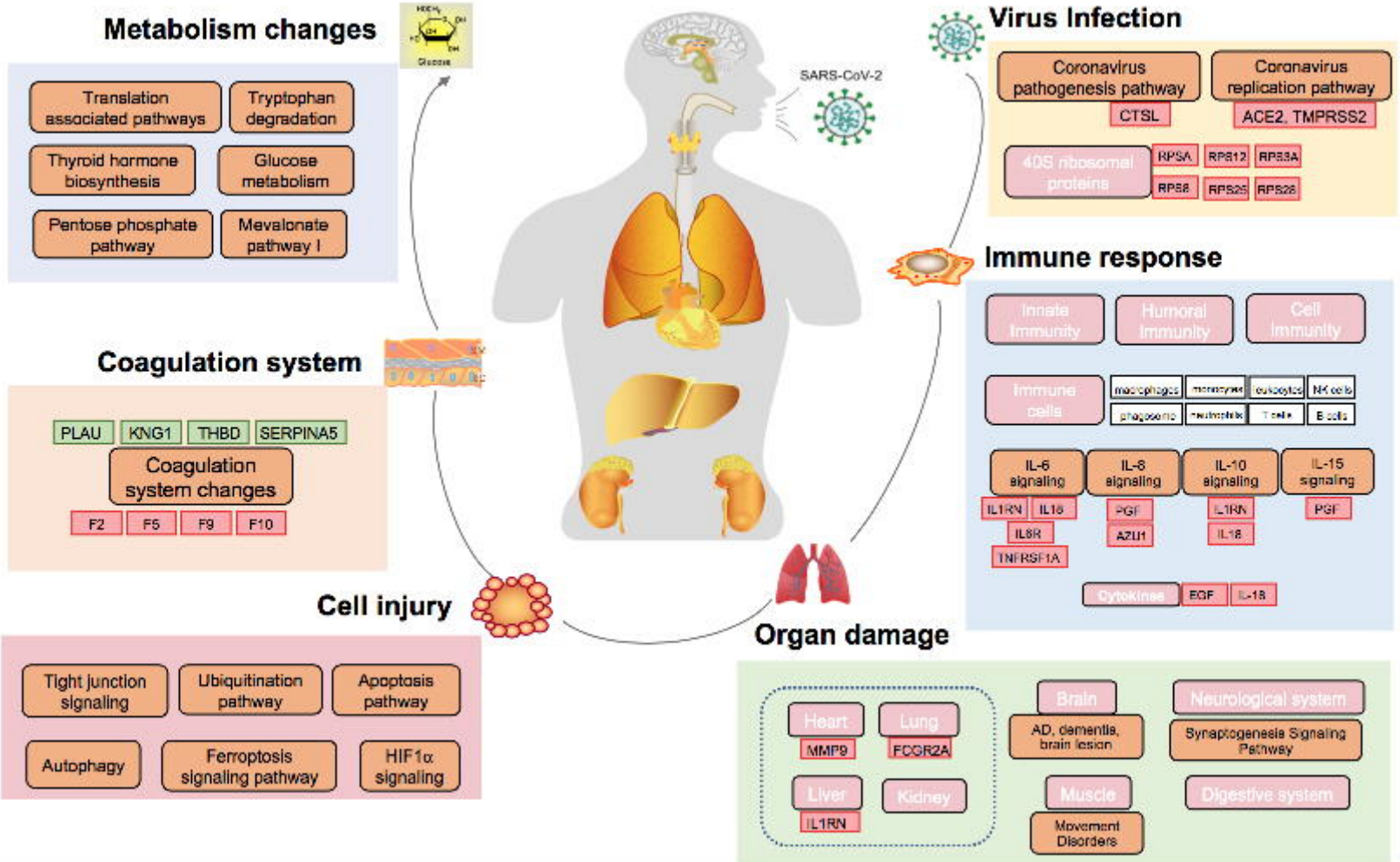
Metabolism changes
Translation associated pathways
Tryptophan degradation
Thyroid hormone biosynthesis
Glucose metabolism
Pentose phosphate pathway
Mevalonate pathway I
Glucose
SARS-CoV-2
Virus Infection
Coronavirus pathogenesis pathway
CTSL
Coronavirus replication pathway
ACE2, TMPRSS2
40S ribosomal proteins
RPSA
RPS12
RPS3A
RPS8
RPS25
RPS28
Immune response
Innate Immunity
Humoral Immunity
Cell Immunity
Immune cells
macrophages
monocytes
leukocytes
NK cells
phagocytes
neutrophils
T cells
B cells
IL-6 signaling
IL-8 signaling
IL-10 signaling
IL-15 signaling
IL1RN
IL18
IL8R
TNFRSF1A
PGF
AZU1
IL1RN
IL18
PGF
Cytokines
EGF
IL-18
Coagulation system
PLAU
KNG1
THBD
SERPINA5
Coagulation system changes
F2
F5
F9
F10
Cell injury
Tight junction signaling
Ubiquitination pathway
Apoptosis pathway
Autophagy
Ferroptosis signaling pathway
HIF1α signaling
Organ damage
Heart
MMP9
Lung
FCGR2A
Liver
IL1RN
Kidney
Brain
AD, dementia, brain lesion
Neurological system
Synaptogenesis Signaling Pathway
Muscle
Movement Disorders
Digestive system